PHYSICAL REVIEW B VOLUME 4, NUMBER 8 15 OCTOBER 1971

# Mixing of Acoustic Waves in Piezoelectric Semiconductors

E. M. Conwell and A. K. Ganguly
*Bayside Research Center, GTE Laboratories Incorporated, Bayside, New York* 11360
(Received 14 April 1971)

The acoustoelectric effect, besides producing linear gain or loss of a single acoustic wave, couples together different acoustic waves. In this paper we first derive expressions for the second-order field acting on a given wave due to acoustoelectric interaction with other waves, either collinear or phase matched (and therefore noncollinear). These fields are obtained also for the case that trapped as well as free carriers are involved in acoustoelectric interaction. The wave equations are then set up for three coupled waves and solved for downconversion and upconversion, with pump depletion due to the interaction with other waves generally, but not always, neglected. In the absence of linear gain or loss, the coupled equations and solutions are quite similar to those of nonlinear optics, with displacements playing the role of electric fields. Many of the results derived in nonlinear optics are therefore easily adapted to the acoustoelectric case. The presence of sizable linear gains or losses, generally different for the different frequencies, changes the form of the solution, and also has the consequence that phase matching loses much of its importance. The dependence of gain rates for downconversion and upconversion on the frequencies of the waves involved, on the applied dc field, on the conductivity of the material, and on the trapping parameters is investigated. Detailed plots are given for some particular cases for which there are experimental data. Finally, the theory is compared with two sets of experimental data: (i) data of Zemon and Zucker, who studied the generation of subharmonics, second harmonics, and sum frequencies by a 1-GHz pump in CdS and (ii) data from many sources on the evolution of the noise frequency spectrum in moving domains in CdS and GaAs. It is found that the theory gives a good qualitative account of many of the observed phenomena.

## I. INTRODUCTION

It is well known that an acoustic wave propagating in a piezoelectric semiconductor will, because of its electric field, give rise to a bunching of the carriers. This bunching results in the familiar attenuation or amplification of the wave, depending on whether the drift velocity of the carriers, in an applied electric field, is smaller or greater, respectively, than the wave velocity.[1] When more than a single wave is present, interactions occur between the different waves because the bunches produced by one wave interact with the electric fields due to other waves or, perhaps more accurately, because electrons are simultaneously bunched by all the waves. To distinguish the attenuation or amplification caused by interactions of different waves from that due to the interaction between a wave and its own bunched carriers, we shall call the latter "linear." In fact, the amplitude of the bunching produced by a single wave is linear in the displacement or strain amplitude for acoustic intensities small enough to bunch only a small fraction of the carriers. In this paper we shall develop the theory for strain amplitudes $\hat{S}$ small enough to lie within this linear regime.[2] How large a strain amplitude this permits depends on the conductivity of the material, the drift field, the frequency, and other parameters. For a shear wave in the basal plane of semiconducting CdS, for example, at the frequency $f_{mg}$ for which the wave creates the maximum bunching (and therefore has the greatest linear gain or loss), $\hat{S} \sim 10^{-5}$ is well within this linear regime. At other frequencies, still higher strains are in the linear regime. For a typical sample of photoconducting CdS smaller strains, of the order of a few times $10^{-6}$, are required to be well within the linear regime at $f_{mg}$. Such strains are large enough to cause a great deal of mixing of waves and harmonic generation.

We begin our discussion in Sec. II by deriving expressions for the field acting on a given wave in the presence of other waves, collinear or phase matched with the first wave. These expressions are derived first for the case of free carriers, then for the case that trapped as well as free carriers participate in the bunching. In Sec. III these fields are used in setting up the wave equations for the case of three coupled waves. The equations are then solved for downconversion, first for the collinear, then for the phase-matched case, with and without trapping. Pump depletion due to the wave interaction is neglected here, but linear attenuation or gain of the pump are included. The ratio of the energies of signal and idler after parametric amplification is considered. In Sec. IV the dependence of parametric gain on the many parameters involved is examined and numerical results presented for some particular cases. Sum frequency for collinear and noncollinear cases and second-harmonic generation are taken up in Sec. V, and the dependence of the latter on the various parameters ex-

amined. A solution that does include pump depletion is given for the case of second-harmonic generation. In Sec. VI we conclude with an extensive comparison of the theory with experimental observations of upconversion and downconversion, including those on propagating acoustic domains.

## II. COUPLING FIELDS

To derive the field acting on one wave due to the presence of other waves, not necessarily collinear, we start from Poisson's equation

$$\nabla\cdot\vec{D}=Q=-qn_s, \tag{2.1}$$

where $n_s$ is the density of electrons producing the space charge, and the equation of current continuity

$$\nabla\cdot\vec{J}=-\frac{\partial Q}{\partial t}. \tag{2.2}$$

The notation and units here are those of Ref. 1 unless otherwise specified. Combining Eqs. (2.1) and (2.2), we obtain

$$\nabla\cdot\left(\vec{J}+\frac{\partial\vec{D}}{\partial t}\right)=0. \tag{2.3}$$

The current density is the sum of conduction and diffusion contributions

$$\vec{J}=nq\mu\vec{E}+q\mathfrak{D}\nabla n, \tag{2.4}$$

where $\mathfrak{D}$ is the diffusion constant and $n$ the local density of electrons in the conduction band. If we allow for trapping, this density is given by[1]

$$n=n_0+fn_s, \tag{2.5}$$

where $n_0$ is the equilibrium density of electrons and $f$ the fraction of the space charge that is free. In going beyond this point, it is convenient to proceed in rather different ways for the cases with and without trapping. We shall carry through the latter first.

### A. Without Trapping

In the absence of trapping, $n$ may be eliminated from Eq. (2.4) by the use of Poisson's equation and (2.5) with $f=1$. Substitution of the result in (2.3) gives the relation between $\vec{D}$ and $\vec{E}$

$$\nabla\cdot\left(\frac{\partial\vec{D}}{\partial t}+\sigma_0\vec{E}-\mathfrak{D}\nabla\nabla\cdot\vec{D}\right)=\nabla\cdot(\mu\vec{E}\,\nabla\cdot\vec{D}), \tag{2.6}$$

where $\sigma_0=n_0q\mu$. This relation[3] constitutes the generalization of White's[1] Eq. (7) to the three-dimensional case without trapping. Assume now that the field and displacement are given by

$$\vec{E}=\vec{E}_0+\frac{1}{2}\sum_{m>0}(\hat{\vec{E}}_m e^{i(\vec{k}_m\cdot\vec{r}-\omega_m t)}+\text{c.c.}), \tag{2.7a}$$

$$\vec{D}=\vec{D}_0+\frac{1}{2}\sum_{m>0}(\hat{\vec{D}}_m e^{i(\vec{k}_m\cdot\vec{r}-\omega_m t)}+\text{c.c.}), \tag{2.7b}$$

where c.c. stands for complex conjugate. The dc terms $\vec{E}_0$ and $\vec{D}_0$ will be assumed, in what follows, to be independent of the amplitudes $\hat{E}_m$ and $\hat{D}_m$ and of space coordinates. $\vec{E}_0$ is then to be identified with the applied dc field. These assumptions are reasonable if the strains are not too large. To obtain the coupling fields, we need also the relation between $\vec{D}$, $\vec{E}$, and the strain $S$, e.g.,

$$\vec{D}=\epsilon\vec{E}+\underline{e}\cdot\vec{\vec{S}}. \tag{2.8}$$

We assume that $S$ may be decomposed into plane waves just as $\vec{E}$ and $\vec{D}$ have been. In the basal plane of CdS, for which we do our calculations, the piezoelectric constant $e$ is independent of direction. We neglect the anisotropy of the dielectric constant $\epsilon$ since, as will be seen, the angular spread we deal with will be small. Substituting (2.7) and (2.8) into (2.6), and assuming as usual that the variation of the wave amplitudes is small in the distance of a wavelength, we find that $\hat{\vec{E}}_m$ may be written in the form

$$\hat{\vec{E}}_m=\hat{\vec{E}}_m^{(1)}+\hat{\vec{E}}_m^{(2)}, \tag{2.9}$$

where $\hat{\vec{E}}_m^{(1)}$ is the familiar result of first-order theory[1]

$$\hat{\vec{E}}_m^{(1)}=-\frac{\underline{e}}{\epsilon}\cdot\frac{\gamma_m+i\omega_m/\omega_D}{\Gamma_m}\hat{\vec{S}}_m. \tag{2.10}$$

Here

$$\gamma_m=2_m(\mu E_0\cos\phi_m)/v_s, \tag{2.11}$$

$\phi_m$ being the angle between $\vec{E}_0$ and $\vec{k}_m$, and

$$\Gamma_m=\gamma_m+i(\omega_c/\omega_m+\omega_m/\omega_D). \tag{2.12}$$

The sign conventions are such that the $-$ sign in $\gamma_m$ applies when electron drift has a component parallel to $\vec{k}_m$, the $+$ sign when it has a component antiparallel to $\vec{k}_m$. As usual, $\omega_c\equiv\sigma_0/\epsilon$, $\omega_D\equiv v_s^2/D$. The higher-order field $\hat{\vec{E}}_m^{(2)}$, containing the terms due to mixing, may be written

$$\hat{\vec{E}}_m^{(2)}=-\frac{\mu}{2\epsilon\omega_m\Gamma_m}\sum_{m'>0}(\vec{D}_{m+m'}\cdot\vec{k}_{m+m'}\hat{\vec{E}}_{m'}^{*}e^{i\Delta_{m+m'}\cdot\vec{r}}+\hat{\vec{D}}_{m-m'}\cdot\vec{k}_{m-m'}\hat{\vec{E}}_{m'}e^{i\Delta_{m-m'}\cdot\vec{r}}), \tag{2.13}$$

where

$$\Delta_{m\mp m'}=\vec{k}_{m\mp m'}-\vec{k}_m\pm\vec{k}_{m'}, \tag{2.14}$$

the subscript $m\pm m'$ denoting the quantity associated with the frequency $\omega_{m\pm m'}$ or $\omega_m\pm\omega_{m'}$, respectively. To write (2.13) as shown the conventions have been used that $D_{-m'}=D_{m'}^{*}$, $k_{-m'}=-k_{m'}$. Note that (2.13) has been simplified somewhat by making the assumption for the first term that $\hat{E}_{m'}^{*}\cdot(\vec{k}_{m+m'}-\vec{k}_{m'})\simeq\hat{\vec{E}}_{m'}^{*}\cdot\vec{k}_m$ and a similar assumption for the second term. This is a good approximation here since, although there is dispersion, it is usually quite

small. This type of approximation is, of course, not permissible in the arguments of the exponentials.

To carry the theory further, it is necessary to insert in (2.13) values for $\vec{D}_{m\pm m'}$ and $\vec{E}_{m'}$. Since we are confining ourselves to the case of not too large strains, or weak interactions, we assume that the relation between $\vec{D}$ or $\vec{E}$ at $\omega_{m'}$ and the strain at $\omega_{m'}$ are the same as in the absence of other waves, i.e., the first-order relation. The resulting $\vec{E}_m^{(2)}$ for many waves has been written down elsewhere.[4]

Here we shall write only the results for three interacting waves, shown in Fig. 1, with wave vectors $\vec{k}_1$ along $x'$, $\vec{k}_2$ along $x''$, and $\vec{k}_3$ along $x$. The highest frequency $\omega_3$ is the sum of $\omega_1$ and $\omega_2$. For Secs. II–IV the electric field $\vec{E}_0$ will be assumed parallel to $\vec{k}_3$, making $\phi_m = \theta_m$. The cases of greatest interest to us are (i) the three waves phase matched, i.e., $\vec{k}_3 - \vec{k}_1 - \vec{k}_2 = 0$, which implies that they are not collinear and (ii) the three waves collinear. For the phase-matched case we obtain from (2.13) for the component of $\vec{E}_1^{(2)}$ parallel to $\vec{k}_1$

$$\hat{E}_1^{(2)} = i\,\frac{e^2\mu}{2\epsilon^2 v_s}\,\frac{\omega_c}{\omega_1}\,\frac{(\gamma_2 - i\omega_2/\omega_D)\cos(\theta_1+\theta_2) + (\gamma_3 + i\omega_3/\omega_D)\cos\theta_1}{\Gamma_1\Gamma_2^*\Gamma_3}\,\hat{S}_2^*\hat{S}_3 . \tag{2.15a}$$

To obtain $\hat{E}_2^{(2)}$ one must replace subscript 1 by 2 and 2 by 1 in (2.15). The component $\hat{E}_3^{(2)}$ parallel to $\vec{k}_3$ is given by

$$\hat{E}_3^{(2)} = i\,\frac{e^2\mu}{2\epsilon^2 v_s}\,\frac{\omega_c}{\omega_3}\,\frac{(\gamma_1 + i\omega_1/\omega_D)\cos\theta_1 + (\gamma_2 + i\omega_2/\omega_D)\cos\theta_2}{\Gamma_1\Gamma_2\Gamma_3}\,\hat{S}_1\hat{S}_2 . \tag{2.15b}$$

For the collinear case, where there is not phase matching,

$$\hat{E}_1^{(2)} = i\,\frac{e^2\mu}{2\epsilon^2 v_s}\,\frac{\omega_c}{\omega_1}\,\frac{2\gamma + i\omega_1/\omega_D}{\Gamma_1\Gamma_2^*\Gamma_3}\,\hat{S}_2^*\hat{S}_3\,e^{i\Delta kx}, \tag{2.16a}$$

$$\hat{E}_3^{(2)} = i\,\frac{e^2\mu}{2\epsilon^2 v_s}\,\frac{\omega_c}{\omega_3}\,\frac{2\gamma + i\omega_3/\omega_D}{\Gamma_1\Gamma_2\Gamma_3}\,\hat{S}_1\hat{S}_2\,e^{-i\Delta kx}\quad(\omega_1 \neq \omega_2), \tag{2.16b}$$

where $\Delta k = k_3 - k_1 - k_2$. For $\omega_1 = \omega_2$, i.e., the degenerate case, $\hat{E}_3^{(2)}$ is smaller by a factor of 2 than the expression obtained from (2.16b) by setting $\omega_1 = \omega_2$. If $\theta_1$ and $\theta_2$ are set equal to zero in (2.15), one obtains the results (2.16), except, of course, for the factors $e^{\pm i\Delta kx}$. In practice, since dispersion is not large, $\hat{E}_1^{(2)}$ and $\hat{E}_3^{(2)}$ of (2.15) are not too different from the coefficients of $e^{i\Delta kx}$ and $e^{-i\Delta kx}$, respectively, in (2.16).

### B. With Trapping

We return now to the case where trapping is present. It was first pointed out by Greebe[5] that the trapping factor $f$ must in general be complex and frequency dependent to allow for the phase difference between free and trapped carriers. Under the assumption that there is a single type of trap, the degree of whose filling can be neglected, it is found[6] that for an acoustic frequency $\omega_m$, $f$ is given by

$$f_m \equiv f(\omega_m) = (f_0 - i\omega_m\tau)/(1 - i\omega_m\tau), \tag{2.17}$$

where $f_0$ is the fraction of its time, in the steady state, spent by a conduction electron on traps and $\tau$ a characteristic trapping time. In detail,[7] $\tau = \tau_f\tau_t/(\tau_f + \tau_t)$, where $\tau_f$ is the mean time an electron is free, $\tau_t$ the mean time spent on a trap before reemission. Note that the right-hand side of (2.17) is the complex conjugate of that given in Refs. 6 and 7, the reason being that we have assumed the conjugate time dependence. The result (2.17) has been found to be in qualitative agreement with experiment for CdS.[6,7]

Because of the frequency dependence of $f$, it is no longer possible to express $n$ simply in terms of $\vec{D}$. Expanding $n$ in the same type of series as used for $\vec{E}$ and $\vec{D}$ in (2.7), and then using Poisson's equation, we obtain for the amplitude at $\omega_m$

$$\hat{n}_m = -ik_m f_m \hat{D}_m/q . \tag{2.18}$$

When (2.7) and (2.8) are inserted in (2.3) and (2.18) used to eliminate $n$, the terms in $e^{-i\omega_m t}$ yield, for

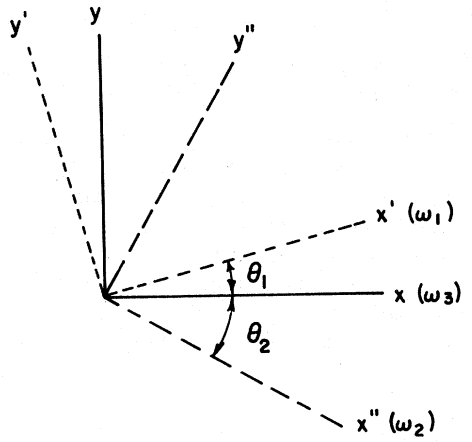


FIG. 1. Propagation directions of three interacting waves.

the first-order field,

$$\hat{E}_m^{(1)} = -\frac{e}{\epsilon}\,\frac{\gamma_m^t + i f_m \omega_m/\omega_D}{\Gamma_m^t}\,\hat{S}_m, \tag{2.19}$$

where

$$\gamma_m^t = 1 \pm (\mu E_0 f_m \cos\theta_m)/v_s \tag{2.20}$$

and

$$\Gamma_m^t = \gamma_m^t + i(\omega_c/\omega_m + f_m \omega_m/\omega_D). \tag{2.21}$$

The second-order field may be obtained from (2.13) by replacing $\hat{D}_{m''}$ with $f_{m''}\hat{D}_{m''}$ and $\Gamma_m$ by $\Gamma_m^t$. Proceeding as in the case without trapping, we obtain for the situation of three collinear waves

$$\hat{E}_1^{(2)} = i\,\frac{e^2\mu}{2\epsilon^2 v_s}\,\frac{\omega_c}{\omega_1}\,\frac{f_2^*\gamma_3^t + f_3\gamma_2^{t*} + i f_2^* f_3 \omega_1/\omega_D}{\Gamma_1^t \Gamma_2^{t*} \Gamma_3^t}\,\hat{S}_2^*\hat{S}_3\, e^{i\Delta kx}. \tag{2.22a}$$

Again, $\hat{E}_2^{(2)}$ is obtained from this by replacing the subscript 1 by 2 and 2 by 1. The second-order field at $\omega_3$ is given by

$$\hat{E}_3^{(2)} = i\,\frac{e^2\mu}{2\epsilon^2 v_s}\,\frac{\omega_c}{\omega_3}\,\frac{f_2\gamma_1^t + f_1\gamma_2^t + i f_1 f_2 \omega_3/\omega_D}{\Gamma_1^t \Gamma_2^t \Gamma_3^t} \times \hat{S}_1\hat{S}_2\, e^{-i\Delta kx} \quad (\omega_1 \neq \omega_2). \tag{2.22b}$$

As in the case without trapping, for $\omega_1 = \omega_2$, $\hat{E}_3^{(2)}$ is $\frac{1}{2}$ of the right-hand side of (2.22b). It is apparent that, in the limit $f_m = 1$, $\hat{E}_1^{(2)}$ and $\hat{E}_3^{(2)}$ go over to (2.16a) and (2.16b), respectively.

## III. DOWNCONVERSION

### A. Wave Equations

We shall write and solve the wave equation only for shear waves with displacement parallel to the $c$ axis. The tensor nature of the elastic constant $c$, as well as that of $\epsilon$ and $e$, may be neglected. The propagation direction of the wave with frequency $\omega_m$ will be denoted by $x_m$. The wave equation for the displacement $\vec{u}_m$ of this wave may then be written

$$\rho\,\frac{\partial^2 u_m}{\partial t^2} - c\,\frac{\partial^2 u_m}{\partial x_m^2} = -e\,\frac{\partial E_m}{\partial x_m} + 2c\alpha_{l,m}\,\frac{\partial u_m}{\partial x_m}, \tag{3.1}$$

where $\rho$ represents the density, $E_{x_m}$ the component of $\vec{E}$ in the $x_m$ direction, and the term $2c\alpha_{l,m}\,\partial u_m/\partial x_m$ the effect of lattice attenuation. This is not the form in which the lattice attenuation is usually written, but it is convenient for our purposes. For the driving field $\hat{E}_{x_m}$ we insert the sum of $\hat{E}_m^{(1)}$ and the appropriate $\hat{E}_m^{(2)}$.

We now look for a solution in the form of a plane wave

$$u_m = \hat{u}_m(x_m)\, e^{i(k_m x_m - \omega_m t)}. \tag{3.2}$$

When (3.2) is substituted into (3.1) and the condition imposed that the change in all quantities is small in a distance of a wavelength, it becomes a first-order differential equation. With (2.10) or (2.19) inserted for $\hat{E}_m^{(1)}$ this equation has one set of terms in phase with $\hat{u}_m$ and another set out of phase with $\hat{u}_m$. Equating the first set to zero, we obtain the dispersion. Making use of the fact that $e^2/\epsilon c$ is small, we may write the dispersion relation, with trapping,

$$\frac{\omega_m}{k_m} \equiv v_s(\omega_m) \simeq \left(\frac{c}{\rho}\right)^{1/2}\left[1 + \frac{e^2}{2\epsilon c}\,\mathrm{Re}\left(\frac{\gamma_m^t + i f_m \omega_m/\omega_D}{\Gamma_m^t}\right)\right]. \tag{3.3}$$

When there is no trapping $f_m = 1$ and (3.3) reduces to the usual linear dispersion[1]

$$v_s(\omega_m) = \left(\frac{c}{\rho}\right)^{1/2}\left\{1 + \frac{e^2}{2\epsilon c}\,|\Gamma_m|^{-2}\left[\gamma^2 + \frac{\omega_m}{\omega_D}\left(\frac{\omega_c}{\omega_m} + \frac{\omega_m}{\omega_D}\right)\right]\right\}. \tag{3.4}$$

In Fig. 2 there are shown some $v_s$ values calculated from (3.3) and (3.4) for shear waves of different frequencies traveling in the basal plane of CdS. The other parameters chosen are ones that will be used in later calculations. In all the cases shown, and indeed universally for $\vec{v}_d$ parallel to $\underline{k}$,[8] $v_s$ decreases monotonically from the stiffened velocity $(c/\rho)^{1/2}(1 + e^2/2\epsilon c)$ in the high-frequency limit to $(c/\rho)^{1/2}$ in the low-frequency limit, where the carriers screen out the electric field produced by the strain (for the parameters used see Table I in Sec. IV). Increasing $\omega_c$, or bringing $\vec{v}_d$ closer to $v_s$ and synchronism, improves the screening and makes the decrease more rapid. In the case shown in Fig. 2(c), with typical values of the trapping parameters, trapping also has the effect of improving the screening. For some other sets of parameters, however, trapping has the opposite effect.

After the terms in the phase with $\hat{u}_1$ have been removed, the remaining terms of (3.1) may be written

$$\frac{d\hat{u}_m}{dx_m} = -(\alpha_{l,m} + \alpha_{e,m})\,\hat{u}_m + \frac{e}{2c}\,\hat{E}_m^{(2)}, \tag{3.5}$$

where $\alpha_{e,m}$ is the linear electronic gain, given by

$$\alpha_{e,m} = -\frac{e^2}{2\epsilon c}\,k_m\,\mathrm{Im}\,\frac{\gamma_m^t + i f_m \omega_m/\omega_D}{\Gamma_m^t}. \tag{3.6}$$

With $f_R$ and $f_I$ representing the real and imaginary parts, respectively, of $f(\omega_m)$, (3.6) may be written[8,9]

$$\alpha_{e,m}^t = \frac{e^2}{2\epsilon c}\,\frac{\omega_c}{v_s}\,\frac{1 \pm f_R(\mu E_0/v_s)\cos\theta_m - f_I(\omega_m/\omega_D)}{[1 \pm f_R(\mu E_0/v_s)\cos\theta_m - f_I(\omega_m/\omega_D)]^2 + [(\omega_c/\omega_m) \pm f_I(\mu E_0/v_s)\cos\theta_m + f_R(\omega_m/\omega_D)]^2}. \tag{3.7}$$

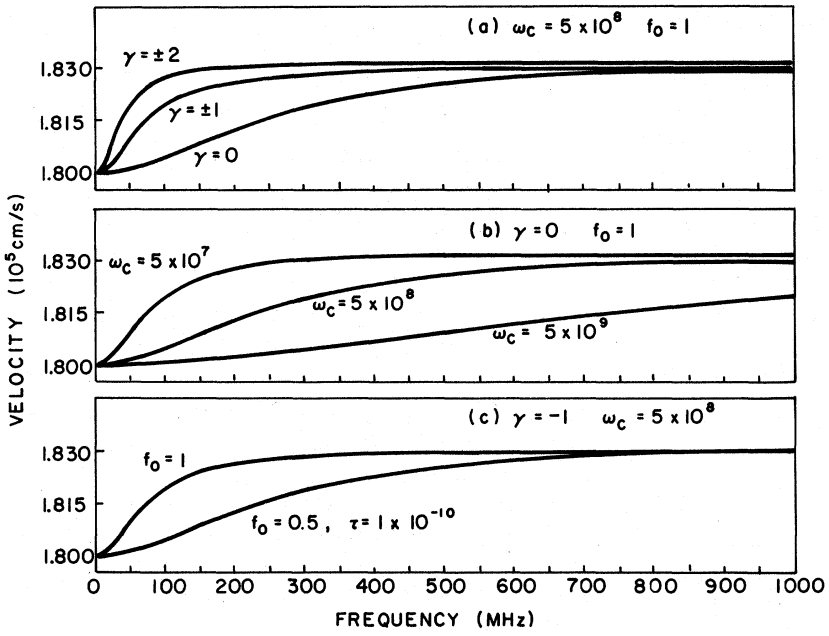


FIG. 2. Dispersion curves for shear waves traveling in the basal plane of CdS for different values of $\omega_c$, $\gamma$, and the trapping parameters.

When trapping is absent, $f_R = 1$, $f_I = 0$, and (3.7) goes over to the usual formula of linear theory.[1] To illustrate the effect of trapping on the linear gain, we have plotted $\alpha_e$ vs $\mu E_0/v_s$ in Fig. 3 for a particular case in CdS, with and without trapping, for the same trapping parameters as were used in Fig. 2(c). It is seen that the magnitude of the loss is usually, although not always, increased by trapping. The gain is greatly decreased for small $v_d/v_s$, as reported earlier,[6] but increased somewhat for large $v_d/v_s$. The latter effect is general and not the result of the particular trapping parameters chosen here. In the limit of large $v_d$ the ratio of $|\alpha_{e,m}|$ with trapping to that without approaches $f_R/(f_R^2+f_I^2)$, which is easily shown to be greater than unity. Of course, the correctness of this conclusion is based on the assumption that small-signal theory is still valid at such large values of $v_d/v_s$.

We shall consider solutions of the Eqs. (3.5) only for the case of three interacting waves. The directions of these waves will be as indicated in Fig. 1. $\vec{E}_0$ will be assumed to lie in the $x$ direction. With the notation

$$\alpha_m \equiv \alpha_{e,m} + \alpha_{l,m}\,, \tag{3.8}$$

the set of equations (3.5) for the three waves may be written

$$\frac{d\hat{u}_1}{dx'} = -\alpha_1\hat{u}_1 + \frac{e}{2c}\hat{E}_1^{(2)}\,, \tag{3.9a}$$

$$\frac{d\hat{u}_2}{dx''} = -\alpha_2\hat{u}_2 + \frac{e}{2c}\hat{E}_2^{(2)}\,, \tag{3.9b}$$

$$\frac{d\hat{u}_3}{dx} = -\alpha_3\hat{u}_3 + \frac{e}{2c}\hat{E}_3^{(2)}\,. \tag{3.9c}$$

These three equations are coupled together by the $\hat{E}^{(2)}$ terms. In this section we shall consider solutions for the case of downconversion, i.e., initial conditions (at $x = 0$) in which the amplitude at $\omega_3$, the highest of the three frequencies, is large while that at either $\omega_1$ or $\omega_2$, or at both, is small. For small $x$ then the product $\hat{u}_1\hat{u}_2$ is small and we may take advantage of this to uncouple (3.9c) by neglecting $\hat{E}_3^{(2)}$. Solutions obtained in this way are of

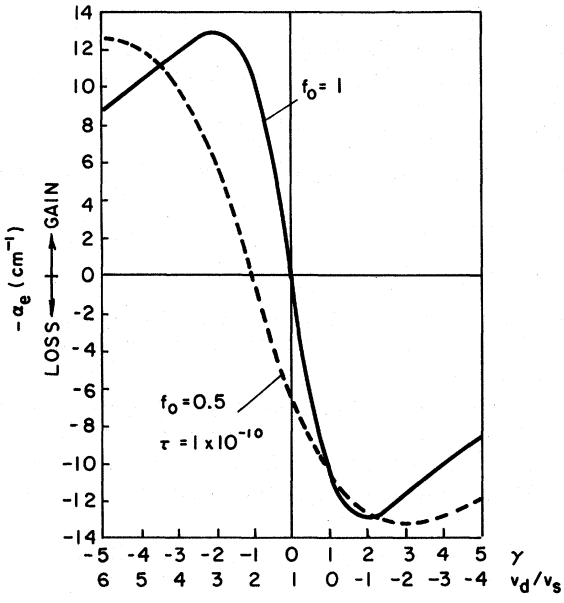


FIG. 3. Linear electronic gain with and without trapping vs $\gamma$ for 42-MHz shear waves in a CdS sample with $\omega_c = 5\times10^8$/sec.

course valid only for values of $x$ small enough so that the depletion of the pump, i.e., $\omega_3$, may be neglected. They are nevertheless useful for getting information about thresholds and about the relative probabilities of different processes. Solutions valid for all $x$ have been obtained for a set of equations rather similar to (3.9), describing three interacting light waves.[10] However, the validity of those solutions is limited to the case that $\alpha$ is the same for all three waves, a relatively infrequent situation for the acoustical problem dealt with here. We have nevertheless included such a solution for the case of second-harmonic generation, which will be taken up in Sec. V.

When $\hat{E}_3^{(2)}$ can be neglected, the solution of (3.9c) is

$$\hat{u}_3 = \hat{u}_3(0)\, e^{-\alpha_3 x}, \tag{3.10}$$

$\hat{u}_3(0)$ being the pump amplitude at $x=0$, which we may choose real. With (3.10) we may proceed to solve (3.9a) and (3.9b) for various cases. The first cases to be considered are those for which $x' = x'' = x$, i.e., collinear cases.

### B. Solution for Collinear Case, $|\alpha_3| x \ll 1$

For the collinear case, (3.9a) and (3.9b) may be written

$$\frac{d\hat{u}_1}{dx} = -\alpha_1 \hat{u}_1 + \eta_1 |S_3(0)|\, e^{-\alpha_3 x}\, e^{i\Delta k x}\, \hat{u}_2^*, \tag{3.11a}$$

$$\frac{d\hat{u}_2^*}{dx} = -\alpha_2 \hat{u}_2^* + \eta_2^* |S_3(0)|\, e^{-\alpha_3 x}\, e^{-i\Delta k x}\, \hat{u}_1, \tag{3.11b}$$

where, in the absence of trapping,

$$\eta_1 = \frac{ie^3\mu}{4\epsilon^2 c v_s}\, \frac{\omega_c}{\omega_1}\, \frac{(2\gamma + i\omega_1/\omega_D)}{\Gamma_1 \Gamma_2^* \Gamma_3}\, k_2 . \tag{3.12a}$$

In the presence of trapping $\eta_1$ is given by

$$\eta_1^t = \frac{ie^3\mu}{4\epsilon^2 c v_s}\, \frac{\omega_c}{\omega_1}\, \frac{f_2^* \gamma_3^t + f_3 \gamma_2^{t*} + i f_2^* f_3 \omega_1/\omega_D}{\Gamma_1^t \Gamma_2^{t*} \Gamma_3^t}\, k_2 . \tag{3.12b}$$

The quantity $\eta_2$ is obtained from (3.12a) or (3.12b) by interchanging subscripts 1 and 2. Consistent with approximations already made, the $\eta$'s are independent of $x$. Since the presence of the factor $e^{-\alpha_3 x}$ complicates solution, we shall solve first for the case $\alpha_3 x \ll 1$, so that $e^{-\alpha_3 x}$ may be replaced by unity. We can then readily eliminate one variable and obtain a second-order differential equation for the other, e.g.,

$$\frac{d^2\hat{u}_1}{dx^2} + (\alpha_1 + \alpha_2 - i\Delta k)\, \frac{d\hat{u}_1}{dx} - (\eta_1\eta_2^* |S_3(0)|^2 - \alpha_1\alpha_2 + i\alpha_1\Delta k)\, \hat{u}_1 = 0. \tag{3.13}$$

The solution to (3.13) may be written

$$\hat{u}_1 = e^{i\Delta k x/2}\, e^{-(\alpha_1+\alpha_2)x/2}\, (4m)^{-1} \{[(2m - \alpha_1 + \alpha_2 - i\Delta k)\hat{u}_1(0) + 2\eta_1 |S_3(0)|\, \hat{u}_2^*(0)]\, e^{mx} + [(2m + \alpha_1 - \alpha_2 + i\Delta k)\hat{u}_1(0) - 2\eta_1 |S_3(0)|\, \hat{u}_2^*(0)]\, e^{-mx}\}, \tag{3.14}$$

where

$$m = \left\{\left[\mathrm{Re}\ \eta_1\eta_2^* |S_3(0)|^2 + \left(\frac{\alpha_1 - \alpha_2}{2}\right)^2 - \left(\frac{\Delta k}{2}\right)^2\right] + i\left(\mathrm{Im}\ \eta_1\eta_2^* |S_3(0)|^2 + \frac{\Delta k}{2}(\alpha_1 - \alpha_2)\right)\right\}^{1/2}. \tag{3.15}$$

By a similar procedure we obtain

$$\hat{u}_2^* = e^{-i\Delta k x/2}\, e^{-(\alpha_1+\alpha_2)x/2}\, (4m)^{-1} \{[2\eta_2^* |S_3(0)|\, \hat{u}_1(0) + (2m + \alpha_1 - \alpha_2 + i\Delta k)\hat{u}_2^*(0)]\, e^{mx} - [2\eta_2^* |S_3(0)|\, \hat{u}_1(0) - (2m - \alpha_1 + \alpha_2 - i\Delta k)\hat{u}_2^*(0)]\, e^{-mx}\}. \tag{3.14'}$$

It is readily checked that in the absence of the pump, i.e., $|S_3(0)| = 0$, $\hat{u}_1$ and $\hat{u}_2^*$ are uncoupled and each takes the form (3.10) as expected.

If $\omega_1 \neq \omega_2$, $m$ is, in general, complex and may be written $m = m' + im''$. When $\omega_1$ is not too different from $\omega_2$, the situation we deal with most frequently, the imaginary term is small and

$$m' \simeq [\mathrm{Re}\eta_1\eta_2^* |S_3(0)|^2 + (\tfrac{1}{2}\{\alpha_1 - \alpha_2\})^2 - (\tfrac{1}{2}\Delta k)^2]^{1/2}.$$

The quantity $m''$ may be thought of as a correction to the wave vector, as are $\pm\frac{1}{2}\Delta k$ in the first factor in $\hat{u}_1$ and $\hat{u}_2^*$, respectively.

### C. Effects of Linear Gain or Loss

When $\alpha_1 = \alpha_2 = 0$, which can be reasonably well approximated for $v_d \simeq v_s$, and also $m'' \ll m'$, the results (3.14) and (3.15) go over to those usually given for the optical case.[11,12] (Of course, displacements are replaced by electric fields there.) The quantity $\eta_m |S_3(0)|$ is to be identified with $i/l_m$, $l_m$ being the interaction length for the wave of frequency $\omega_m$.[11] It follows that various results familiar from nonlinear optics may be brought over for this case. Thus, if $m'$ is real, which means here $\mathrm{Re}\eta_1\eta_2^* |S_3(0)|^2 > (\frac{1}{2}\Delta k)^2$, at large enough $x$ (provided,

of course, pump depletion is still negligible) there is exponential growth of the signal and idler as $e^{m'x}$. This is true, independent of initial conditions, for the nondegenerate case. The initial rates of growth of signal and idler may be quite different, however, for some sets of initial conditions. For example, if a sizable signal is introduced but the idler is initially zero, the idler will begin to grow as $\sinh m'x$, whereas the signal, varying as $\cosh m'x$, will not grow at first. In the degenerate case, however, even for $\Delta k = 0$ there will be some particular initial phase difference between the pump and the subharmonic for which the signal will decay exponentially rather than grow. It may be noted that the condition $\mathrm{Re}\eta_1\eta_2^* |S_3(0)|^2 > (\frac{1}{2}\Delta k)^2$ is easier to satisfy in our case than in the optical case because the basic nonlinearity is larger. If the condition is not satisfied, however, $m'$ is imaginary and the amplitudes $\hat{u}_1$ and $\hat{u}_2$ will vary in an oscillatory manner with increasing $x$. As shown by Armstrong *et al.*[10] this corresponds to energy being fed back and forth between the pump on the one hand and signal and idler on the other.

The presence of linear gain or loss alters the situation markedly. If there is gain, i.e., $\alpha_1 + \alpha_2 < 0$, the signal will grow essentially exponentially whether or not $|S_3(0)|$ is large enough to give $m$ a real part. The reason for this, of course, is that there is an additional source of energy, the dc power supply. If $m$ were pure imaginary, the presence of the factor $e^{\pm im''x}$ would simply superimpose ripples on the exponential growth, large for small $|\alpha_i|x$, but ultimately small in effect. If, on the other hand, $\alpha_1 + \alpha_2 > 0$, for the signal to have net gain $|S_3(0)|$ would have to be high enough to overcome the linear loss as well as the effect of $\Delta k$. In all, in the presence of linear gain or loss phase matching becomes much less important.

### D. Weak Coupling

Rather different behavior from that described above may be obtained for the case of weak coupling, i.e.,

$$\mathrm{Re}\eta_1\eta_2^* |S_3(0)|^2 \ll \tfrac{1}{4}(\alpha_1 - \alpha_2)^2 . \tag{3.16}$$

If we neglect $\mathrm{Im}\eta_1\eta_2^* |S_3(0)|^2$ and $\Delta k$, for simplicity, we may expand $m$ to obtain

$$m \simeq \frac{\alpha_1 - \alpha_2}{2}\left(1 + \frac{2\eta_1\eta_2^* |S_3(0)|^2}{(\alpha_1 - \alpha_2)^2}\right) \equiv \frac{\alpha_1 - \alpha_2}{2} + g. \tag{3.17}$$

For an initial condition $\hat{u}_2^*(0) = 0$ we find, using (3.14),

$$\hat{u}_1 \simeq \hat{u}_1(0)\left[\frac{g}{\alpha_1 - \alpha_2} e^{gx} e^{-\alpha_2 x} + \left(1 - \frac{g}{\alpha_1 - \alpha_2}\right) e^{-gx} e^{-\alpha_1 x}\right]. \tag{3.18}$$

As expected, if $|S_3(0)|$ is set equal to zero the first term vanishes and the large square brackets becomes $e^{-\alpha_1 x}$. Assume now that $\alpha_2$ is negative and $|\alpha_2| \gg |\alpha_1|$, so that by (3.16) and some of our later assumptions, $|\alpha_2| \gg \mathrm{Re}(\eta_1\eta_2^*)^{1/2} |S_3(0)|$. Then if $|S_3(0)| \neq 0$, even if it is quite small, the over-all growth of the signal in a long enough crystal will be predominantly as the first term in the large square bracket. In other words, the signal will grow at a rate determined by $|\alpha_2|$ rather than $\alpha_1$. This was first pointed out by Gulayev and Zil'berman,[13] who called it "superheterodyne amplification." They suggest that this effect has been observed experimentally but this is not likely, at least not in the experiments cited,[14] because the condition (3.16) was not realized. Rather these experiments appear to illustrate parametric amplification plus mixing of many frequencies in the presence of linear gain and absence of phase matching.

By somewhat similar considerations to those above, Bloembergen[15] has shown for a weak-coupling case in which, without the pump, there is loss at both the signal and idler frequencies, but the loss rate is very much greater for the idler, that it is possible to obtain net gain for the signal even though the idler is strongly attenuated.

### E. Solution for Collinear Case, Arbitrary $|\alpha_3|x$

We consider now the solution of Eqs. (3.11) when the approximation $|\alpha_3|x \ll 1$ is not made. To show most simply what is involved, let us assume $\Delta k = 0$ and $\omega_1 = \omega_2$. The solution that is then obtained for $\hat{u}_1$ may be written

$$\hat{u}_1 = e^{-\alpha_1 x}\left(Ae^{-\mathcal{F}|\eta_1||S_3(0)|x} + Be^{\mathcal{F}|\eta_1||S_3(0)|x}\right), \tag{3.19}$$

where

$$\mathcal{F} \equiv (1 - e^{-\alpha_3 x})/|\alpha_3|x, \tag{3.20}$$

$A$ and $B$ are arbitrary constants, and $|\eta_1|$ is written for the degenerate case. To understand what (3.19) means physically, consider first the case of linear loss, i.e., $\alpha_1, \alpha_3 > 0$. In the limit $x \to 0$, $\mathcal{F} \to 1$ and (3.19) $\to$ (3.14), written for the degenerate case. If $|\eta_1| > \alpha_1$ there will for small enough $x$ be net gain at the subharmonic, the $B$ term growing exponentially. With increasing $x$, $\mathcal{F}$ decreases monotonically, approaching the value zero in the limit $x \to \infty$. The rate of gain will decrease therefore with increasing $x$, reaching zero at the value of $x$ for which $\mathcal{F}|\eta_1||S_3(0)| = \alpha_1$ (provided, of course, the sample is long enough). If pump depletion due to amplification of the signal and idler had also been included, zero gain would have been reached at a smaller $x$ value. If, on the other hand, the $\alpha$'s had been negative, $-\mathcal{F} = 1$ for $x = 0$ and $-\mathcal{F}$ increases monotonically with increasing $x$. The $A$ term in (3.19) is then the dominant one at large $x$. Parametric gain increases with increasing $x$, as expected

because of the growth of the pump. Note, however, that for $\alpha_3 < 0$ the quantity that appears in the exponent $-\mathfrak{F}|S_3(0)|$ is less than the local value of $|S_3|$, $|S_3(0)|e^{-\alpha_3 x}$. Correspondingly, for $\alpha_3 > 0$ the quantity in the exponent,

$$\mathfrak{F}|S_3(0)| > |S_3(0)|e^{-\alpha_3 x}.$$

These features are easily understood to result from the amplification taking place over a distance. Again, if there were pump depletion due to the parametric process this would cut down the rate of increase of parametric gain.

For the nondegenerate case the solutions do not take as simple a form as (3.19). They can be written in terms of half-integral Bessel functions. The conclusions that linear pump loss (gain) progressively decreases (increases) the rate of parametric gain of the signal must still be valid, however.

### F. Noncollinear Phase-Matched Case

To treat the noncollinear case we return to Eqs. (3.9). Again, the calculations will be simplified by neglecting pump depletion by the parametric process and, initially, changes in the pump amplitude due to linear gain or loss. When (2.15a) is inserted for $\hat{E}_1^{(2)}$ and the appropriate modification of (2.15a) for $\hat{E}_2^{(2)}$, there result equations similar to (3.11), with $\Delta k$ and $\alpha_3 x$ set equal to zero, and $x$ and $\eta_1$ in (3.11a) replaced by $x'$ and $\eta_1'$, $x$ and $\eta_2$ in (3.11b) replaced by $x''$ and $\eta_2'$. Without trapping we have

$$\eta_1' = \frac{ie^3\mu}{4\epsilon^2 c v_s}\frac{\omega_c}{\omega_1}\frac{(\gamma_2 - i\omega_2/\omega_D)\cos(\theta_1+\theta_2) + (\gamma_3 + i\omega_3/\omega_D)\cos\theta_1}{\Gamma_1\Gamma_2^*\Gamma_3}\,k_2 \tag{3.21}$$

and $\eta_2'$ is as usual obtained from $\eta_1'$ by interchanging subscripts 1 and 2. Eliminating $\hat{u}_2^*$ from the coupled equations, we get a differential equation for $\hat{u}_1$ similar to (3.13) except, of course, that derivatives are taken with respect to $x'$ or $x''$ rather than $x$. When $x'$ and $x''$ are expressed in terms of $x$ and $y$ (see Fig. 1), all but one of the terms in the resulting partial differential equation involve derivatives of either $x$ or $y$ alone. The exception is $\sin(\theta_1 - \theta_2)\,\partial^2\hat{u}_1/\partial x\partial y$. This term vanishes for the degenerate case and is small otherwise since $\theta_1$ and $\theta_2$ are small. We may therefore neglect this term and readily solve the remaining equation by separation of variables. The result is[16]

$$\hat{u}_1 = e^{-\alpha_1 x/2\cos\theta_1}\,e^{-\alpha_2 x/2\cos\theta_2}\,[Ae^{qx} + Be^{-qx}], \tag{3.22}$$

where

$$q = \left[\frac{\eta_1'\eta_2'^*|S_3(0)|^2}{\cos\theta_1\cos\theta_2} + \left(\frac{\alpha_1}{2\cos\theta_1} - \frac{\alpha_2}{2\cos\theta_2}\right)^2\right]^{1/2}. \tag{3.23}$$

There is a similar solution for $\hat{u}_2^*$.

The effect of linear gain or loss of the pump is quite similar here to what it was for the collinear case. For $\omega_1 = \omega_2$ the solution for arbitrary $\alpha_3 x$ is

$$\hat{u}_1 = e^{-\alpha_1 x/\cos\theta_1}\,(Ae^{-\mathfrak{F}|\eta_1'||S_3(0)|x/\cos\theta_1} + Be^{\mathfrak{F}|\eta_1'||S_3(0)|x/\cos\theta_1}), \tag{3.24}$$

where $\mathfrak{F}$ is the function defined in (3.20).

### G. Some Energy Relations

It is of interest to compare the energy gained by signal and idler. Clearly when $\alpha \neq 0$ the Manley-Rowe relations do not apply.[17] For simplicity we shall consider the collinear case with $\Delta k = 0$, at large enough $mx$ so that only the $e^{+mx}$ terms need be considered. For that case we obtain from (3.14) and (3.14′) the ratio of energy $\mathcal{E}$ at $\omega_2$ to that at $\omega_1$:

$$\frac{\mathcal{E}(\omega_2)}{\mathcal{E}(\omega_1)} \to \frac{\omega_2^2}{\omega_1^2}\left|\frac{m + \frac{1}{2}(\alpha_1 - \alpha_2)}{\eta_1|S_3(0)|}\right|^2 \quad (mx \gg 1). \tag{3.25}$$

This is then the generalization of the Manley-Rowe relations for this case. If we set $\gamma = 0$ and neglect lattice losses, which are generally small, $\alpha \simeq 0$ and (3.25) goes over to the usual relation[17]

$$\mathcal{E}(\omega_2)/\mathcal{E}(\omega_1) \to \omega_2/\omega_1 \quad (mx \gg 1,\ \alpha = 0). \tag{3.26}$$

## IV. GAIN RATES AND THRESHOLD FOR DOWNCONVERSION

It is apparent from Sec. III that parametric amplification or downconversion by the acoustoelectric mechanism is a complex phenomenon in that there are many variables upon which the ultimate gain or loss of a signal depends. Of the materials parameters, once the material and orientation have been specified the significant variables remaining are $\omega_c$ and the trapping parameters $f_0$ and $\tau$. Apart from the material there are four important parameters—the pump and signal frequencies, the pump power, and $\vec{E}_0$. We shall examine the dependence on all these parameters, providing some numerical results for shear waves propagating in the basal plane of CdS. Most of the plots will be for parameter values for which there are experimental data. Detailed comparison with experiment will be carried out in Sec. VI. Numerical values of various quantities used in the calculations are listed in Table I.

### A. Variation of $\eta$ with $\omega_1$, $\gamma$

Before discussing over-all gain or loss it is useful to study the variation of $\eta$ with the various parameters. Consider first the frequency dependence

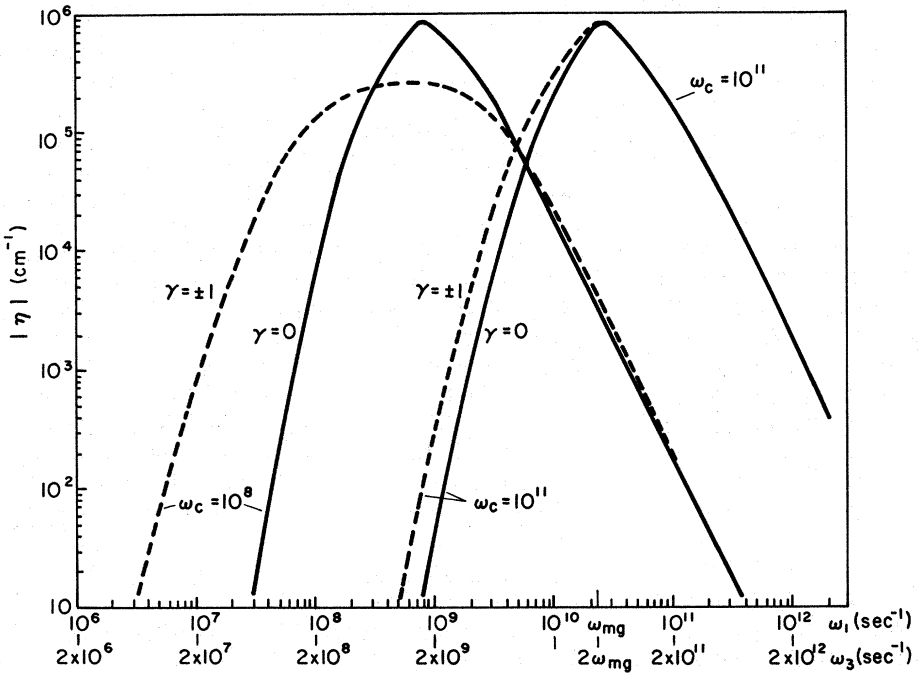


FIG. 4. $|\eta|$ vs pump and subharmonic frequencies for different values of $\omega_c$ and $\gamma$. $\omega_{mg}$ represents the frequency of maximum linear gain for $\omega_c=10^{11}$/sec.

of $\eta_1\eta_2^*$. In the simplest case, $\omega_3=2\omega_1=2\omega_2$ and no trapping, $\eta_1\eta_2^*=|\eta|^2$, where

$$|\eta|=\frac{e^3\mu}{4\epsilon^2cv_s^2}\frac{\omega_c}{\gamma^2+(\omega_c/\omega_1+\omega_1/\omega_D)^2}\times\left(\frac{4\gamma^2+\omega_1^2/\omega_D^2}{\gamma^2+(\omega_c/2\omega_1+2\omega_1/\omega_D)^2}\right)^{1/2}. \quad (4.1)$$

A question of interest is for what value of pump frequency is $|\eta|$ a maximum. For $\gamma=0$ this is readily determined analytically. It is found that $|\eta|$ peaks at $\omega_3=2.34\omega_{mg}$, or $\omega_1=1.17\omega_{mg}$, where $\omega_{mg}=(\omega_c\omega_D)^{1/2}$. The fact that $|\eta|$ peaks at a higher frequency than $\omega_{mg}$, where $|\alpha_e|$ has its maximum (for $\gamma\neq0$),[1] is due to the factor $\omega_1/\omega_D$ in the numerator. For $\gamma\neq0$ the peak in $|\eta|$ is changed little so long as $\gamma^2\ll\omega_1^2/\omega_D^2$. This can be seen in Fig. 4, where $|\eta|$ is plotted versus signal and pump frequencies for some different $\gamma$ values and for $\omega_c=10^8$/sec, representing a typical photoconducting sample, and $\omega_c=10^{11}$/sec, representing a semiconducting sample. It is only for the smaller values of $\omega_1$ and $\omega_3$ that there is a significant difference between the curves for the different $\gamma$'s. The rapid decrease of $|\eta|$ as the pump frequency falls below $\omega_{mg}$ will be seen to have significant consequences for the frequency changes that take place in domains.

The variation of $|\eta|$ with $\gamma$ can be seen more clearly in Fig. 5. Figure 5(a) is a case of a relatively low signal frequency (42 MHz) for which $\omega_1/\omega_D=0.05$. Because of the proportionality of $|\eta|$ to $(4\gamma^2+\omega_1^2/\omega_D^2)^{1/2}$, this results in very low values of $|\eta|$ in the range $\gamma^2\ll(\omega_1/\omega_D)^2$ for the case without trapping, $f_0=1$. In Fig. 5(b) the dip at $\gamma=0$ is much less pronounced because the signal frequency is 495 MHz, for which $\omega_1/\omega_D=0.6$.

The above remarks are made concerning $|\eta|$ for the collinear case. For noncollinear cases the waves were phase matched using (3.3) or (3.4) as necessary. Since, as noted before, dispersion is relatively small, the remarks made so far in this section about $|\eta|$ apply with little modification to phase-matched subharmonic generation in the absence of trapping. They do not necessarily apply to cases with trapping, however. When there is trapping it is useful to consider two limiting cases. In the high-frequency limit $\omega\tau\gg1$, $f_R\to1$, $f_I\to0$. In this limit $|\eta^t|$ values differ little from those of

TABLE I. Parameters for shear waves in basal plane of CdS.

| | |
|---|---|
| $e$ | 0.218 c/m$^2$ [a] |
| $\epsilon/\epsilon_0$ | 9.35 [a] |
| $e^2/2\epsilon c$ | 0.018 [b] |
| $(c/\rho)^{1/2}$ | $1.8\times10^5$ cm/sec [b] |
| $\mu$ | 250 cm$^2$/v sec [c] |
| $\omega_D$ | $5\times10^9$/sec [b] |
| $\alpha_l$ | $6.22f^{1.46}$ Np/cm ($f$ in GHz) [d] |

[a]D. Berlincourt, H. Jaffe, and L. R. Shiozawa, Phys. Rev. 129, 1009 (1963).

[b]A. R. Hutson and D. L. White, J. Appl. Phys. 33, 1 (1962).

[c]Somewhat higher values of $\mu$ were used when warranted for a particular sample.

[d]Taken from the data of T. B. Bateman and J. H. McFee, J. Appl. Phys. 39, 4471 (1968).

$|\eta|$ and the remarks made above about $|\eta|$ are valid for $|\eta^t|$. In the limit $\omega\tau \ll 1$, $f_R \to f_0$, and again $f_I \to 0$. In that limit we may write, for collinear case,

$$|\eta^t| \to \frac{e^3\mu}{4\epsilon^2 c v_s^2} \frac{\omega_c f_0}{(\gamma^t)^2 + (\omega_c/\omega_1 + f_0\,\omega_1/\omega_D)^2} \left( \frac{(2\gamma^t)^2 + (f_0\,\omega_1/\omega_D)^2}{(\gamma^t)^2 + (\omega_c/2\omega_1 + f_0\,2\omega_1/\omega_D)^2} \right)^{1/2} \quad (\omega\tau \ll 1), \tag{4.2}$$

with $\gamma^t = 1 - f_0\, v_d/v_s$ here. As in the case without trapping, for $\omega_1 \ll \omega_D$ this has a steep narrow minimum, shifted however to $1 - f_0\, v_d/v_s = 0$. This is shown in Fig. 5(a) for $\tau = 10^{-10}$, $\omega\tau = 0.0264$. The location of the minimum, since $f_0 = 0.05$, is at $v_d = 2v_s$. From Eq. (3.7) it is found that, in general, $\alpha_e^t$ goes through zero at the $v_d$ value for which $|\eta^t|$ is a minimum. An example of this may be seen by comparing Figs. 3 and 5(a), which are plotted for the same values of the parameters. The minimum of $|\eta^t|$ is smaller than that of $|\eta|$ because of the factors $f_0$ in the numerator of the former. These factors in the numerator account for $|\eta^t|$ being less than $|\eta|$ over a good deal of the range of $\gamma$ shown. For large $|v_d|$, however, the $f_0$ factors in the denominator become predominant and $|\eta^t|$ is larger than $|\eta|$, as seen in the plots. For intermediate values of $\omega\tau$ it is difficult to make any general statements. In numerical calculations we found that as $\omega\tau$ increased from 0.0264 the minimum in $|\eta^t|$ moved from $\gamma = -1$ toward 0, approaching very close to zero for $\omega\tau \geq 2.64$. At $\omega\tau = 0.264$, shown by the dotted curve in Fig. 5(a), the movement was quite significant. The peak values of $|\eta^t|$ were always less than those of $|\eta|$.

In Fig. 5(b), where the pump frequency is close to 1 GHz, and the other parameters the same as in 5(a) except for $\tau$, the minimum in $|\eta^t|$, as well as that in $|\eta|$, is much shallower because of the larger $\omega_1/\omega_D$ value. Since $\omega\tau \ll 1$, the minimum of $|\eta^t|$ occurs at $\gamma = -1$. Interestingly, at this frequency for the $\tau$ value shown (thus, in general, for the $\omega\tau \ll 1$ limit) the peak of $|\eta_1^t|$ is actually higher than that of $|\eta|$. This was not the case for larger values of $\omega\tau$ for which calculations were done at this signal frequency.

The next question one could ask about $|\eta_1\eta_2^*|$ is how its value changes when $\omega_1$ and $\omega_2$ are allowed to vary separately with $\omega_3$ fixed. This is a more difficult situation to get general results for analytically but some may be obtained nevertheless. It is found that, for a wide range of pump frequencies and $\gamma$'s, the highest value of $|\eta_1\eta_2^*|$ occurs at the subharmonic. This is easily verified for $\gamma = 0$ and $\omega_3 \ll \omega_{mg}$. In that case the effect of diffusion is negligible and the terms $\omega_i/\omega_D$ in the denominator may be dropped. The resulting $\mathrm{Re}(\eta_1\eta_2^*) \propto \omega_1^3\omega_2^3$, which has a maximum for $\omega_1 = \omega_2$. In the opposite limit, when all three frequencies are much greater than $\omega_{mg}$, the terms $\omega_c/\omega_i$ in the denominator may be dropped. With $\gamma = 0$ one then obtains $\mathrm{Re}(\eta_1\eta_2^*) \propto (\omega_1\omega_2)^{-1}$. This has a minimum at $\omega_1 = \omega_2$. Analytically it is found that, for $\gamma = 0$, $\mathrm{Re}(\eta_1\eta_2^*)$ peaks at the subharmonic for $\omega_3 < 6\omega_{mg}$, elsewhere for $\omega_3 > 6\omega_{mg}$. In the latter case the deleterious effect of diffusion is apparently lessened if one of the frequencies is lower than $\frac{1}{2}\omega_3$ and the other higher. For $\gamma \neq 0$ it is to be expected that the subharmonic will be favored to even higher pump frequencies and numerical calculations confirm this. Since in practice it has been rare to have a pump frequency much higher than $\omega_{mg}$, the rate of gain has generally been greatest at the subharmonic.

When trapping is included it becomes much more difficult to make any general statements about frequency dependence. Numerical calculations show that $\mathrm{Re}(\eta_1^t\eta_2^{t*})$ peaks very frequently at the subharmonic. However, for some $f_0$ and $\tau$ values $\mathrm{Re}(\eta_1^t\eta_2^{t*})$ peaks off the subharmonic at frequencies where both $\mathrm{Re}(\eta_1\eta_2^*)$ for $f_0 = 1$ and $\mathrm{Re}(\eta_1^t\eta_2^{t*})$ for some other values of $f_0$ and $\tau$ have their maxima at the subharmonic.

### B. Rates of Growth—Phase Matched

We consider now rates of growth or loss of a signal, with the restriction of negligible pump deple-

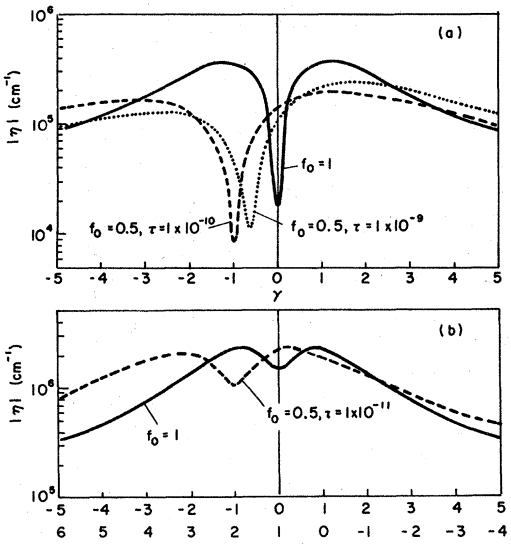


FIG. 5. $|\eta|$ or $|\eta^t|$ vs $\gamma$ for (a) $\omega_1 = 2\pi \times 42 \times 10^6$/sec, $\omega_c = 5 \times 10^8$/sec; (b) $\omega_1 = 2\pi \times 495 \times 10^6$/sec, $\omega_c = 1.68 \times 10^9$/sec, and trapping parameters as indicated.

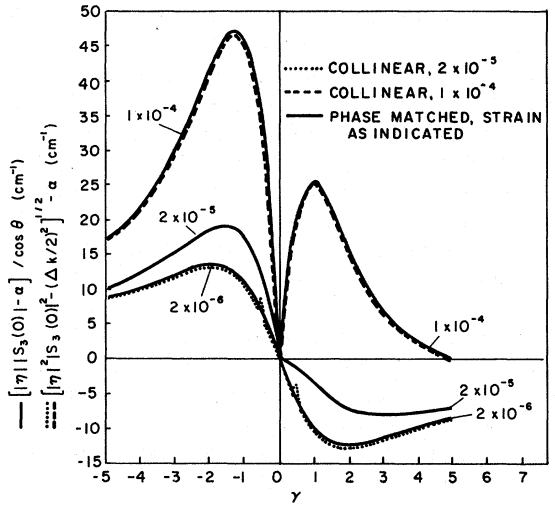


FIG. 6. Net gain vs $\gamma$ for 42-MHz shear waves pumped at 84 MHz, under phase-matched or collinear conditions, with the strains indicated. $\omega_c = 5\times10^8$/sec and no trapping was assumed.

tion, first for phase-matched conditions. In Fig. 6 are shown the sum of linear and parametric gains for some cases of subharmonic generation without trapping. The solid lines are plots of $q - \alpha/\cos\theta$ where, by the definition in (3.23), $q = |\eta|\,|S_3(0)|/\cos\theta$. $\theta$, the phase-matching angle, is typically 3° to 6° for these plots. For a pump strain of $2\times10^{-6}$ the effect of the pump is almost negligible and the curve is essentially $\alpha$ vs $\gamma$. Since lattice loss is small at 42 MHz, this curve is little different from $\alpha_e$ vs $\gamma$, as can be seen by comparing it with the curve of Fig. 3 plotted for the same parameters. For $2\times10^{-5}$ the parametric gain is no longer negligible, as is evidenced by the asymmetry of the curve. With an increase in strain to $10^{-4}$ the exponent is positive everywhere except for a small region near $\gamma = 5$. It should be noted that the strain of $10^{-4}$ has been included for illustrative purposes only; the theory is not expected to be valid for such high strains with $\omega_c = 5\times10^8$/sec.

Qualitatively similar behavior can be seen in Fig. 7 for the phase-matched case with trapping, except that the gain goes through zero at $\gamma = -1$. This, of course, was to be expected since $|\eta^t|$ and $\alpha_e$, as shown in Figs. 5(a) and 3, respectively, are both small around $\gamma = -1$. As a result of this, and also the somewhat different shapes of $\alpha$ and $\eta$ with trapping present, the peak gain occurs for $v_d \simeq 5v_s$, whereas without trapping, it occurs at $v_d \simeq 2.5v_s$. (As usual, these statements will only be true if large amplitude effects can be neglected at the $v_d$'s concerned.) The magnitude of the peak gain is also considerably smaller for the case with trapping. Although no experiments involving parametric amplification of bulk acoustic waves in samples with traps have been reported, there have been such experiments with surface waves.[18] The pump frequency in these experiments was 84 MHz, the signal frequency 42 MHz, and $\omega_c$ was $5\times10^8$/sec, the same values as have been used in our calculations. Detailed results need not be the same for surface waves as for bulk waves, of course, but it is reasonable to expect similar trends. It was generally found with the surface waves[19] that total gain, i.e., including parametric) was quite small until drift velocities as high as $2v_s$ were attained, whereas for bulk experiments where trapping was not present smaller $v_d$'s sufficed. The gains were also much smaller[18] than predicted theoretically by a calculation[20] for surface wave parametric amplification not including trapping. In the light of the results we have just presented, the discrepancy between theory and experiment could be at least partly due to the presence of trapping.

At a pump frequency of 1 GHz and signal frequency of 0.5 GHz, with somewhat larger $\omega_c$, the gains are generally larger, as shown in Fig. 8. The behavior for the phase-matched case at the lower strain values is quite similar to what it was for the lower pump frequency. As in that case, at $2\times10^{-6}$ there is little parametric amplification. At the

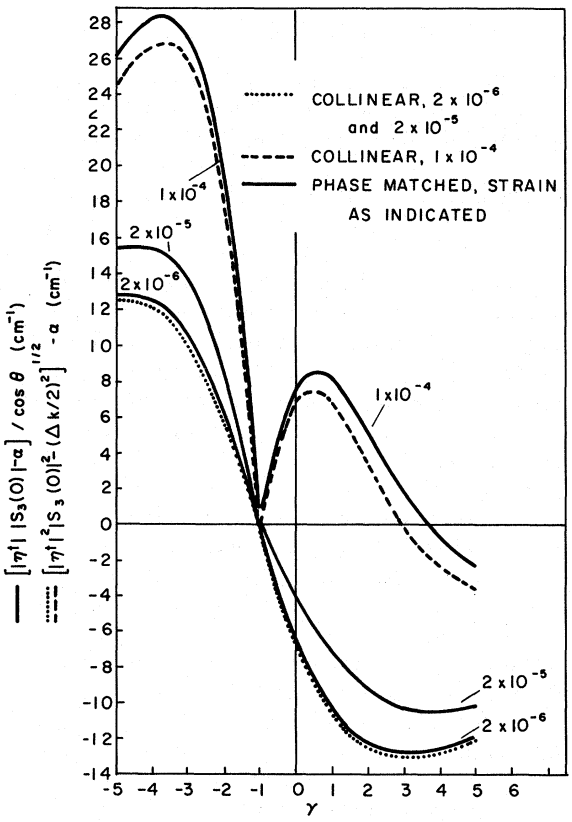


FIG. 7. Same as Fig. 6 except for the incorporation of trapping, with $f_0 = 0.5$, $\tau = 1\times10^{-10}$ sec.

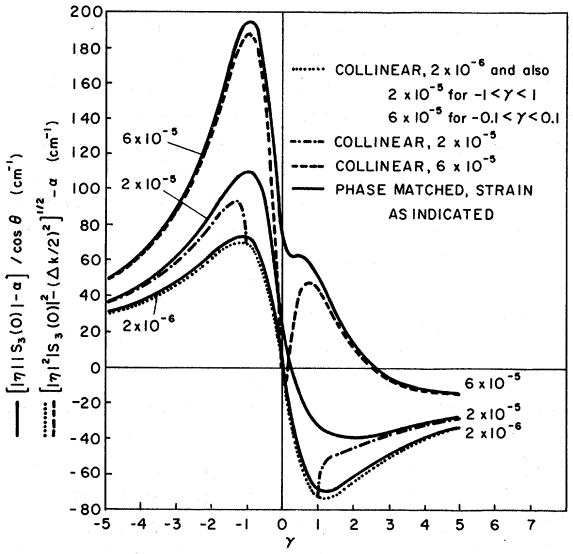


FIG. 8. Net gain vs $\gamma$ for 495-MHz shear waves pumped at 990 MHz, under phase-matched or collinear conditions, with the strains indicated. $\omega_c = 1.68\times10^9$/sec and no trapping was assumed.

highest strain, however, where the parametric gain is the predominant one, the deep minimum at $\gamma = 0$ is replaced by a shallow minimum at $\gamma = 0.2$.

### C. Rates of Growth—Collinear

To understand the way in which rates of growth for the collinear case differ from those for the phase-matched case, we must first consider the variation of $\Delta k$ with the relevant parameters. For the degenerate case ($\omega_1 = \omega_2$) it is readily shown that

$$\Delta k = -k_3(v_3 - v_1)/v_1 \,. \tag{4.3}$$

Plots of $\Delta k$ vs $\gamma$ for some of the cases we have been discussing are shown in Figs. 9(a) and 9(b). It is noted that $|\Delta k|$ is a minimum at $\gamma = 0$ for an 84-MHz pump (without trapping) and a maximum at this $\gamma$ for a 1-GHz pump. Both of these facts are seen to be consistent with the variations of phase velocity shown in Figs. 2(a) and 2(b). The large $\Delta k$ for small $\gamma$ at 1 GHz results from the large $k_3$.

To simplify comparison of gains for the collinear case with those for the phase-matched case, the former were plotted also in Figs. 6–8. For all three cases plotted it is easily deduced from Figs. 5 and 9 that for the smallest strain, $2\times10^{-6}$, $|\eta||S_3(0)| < \frac{1}{2}\Delta k$ and the presence of the pump makes no contribution to growth when the waves are all collinear. For the 84-MHz pump at $2\times10^{-5}$, shown in the dotted line in Fig. 6, only for small regions around $\gamma = \pm 0.5$ (near where $|\eta|$ peaks) does the presence of the pump result in a small real positive contribution to the exponent. Apart from these two small "windows," the exponent for this strain, in the collinear case, is simply $-\alpha$, as it is also for smaller strains. At $1\times10^{-4}$, however, $|\eta||S_3(0)|$ is so much larger than $\frac{1}{2}\Delta k$, except at $\gamma \simeq 0$ where $|\eta|$ has its minimum, that the lack of phase matching has little effect on the gain. With trapping present, as shown in Fig. 7, the same trends are observed although the details are different. There are no longer any "windows" at $2\times10^{-6}$ and the curves for $2\times10^{-6}$ and $2\times10^{-5}$ are coincident everywhere, both representing $-\alpha$ vs $\gamma$.

For the higher pump frequency, shown in Fig. 8, lack of phase matching affects the gain rather differently. For large $|\gamma|$ values its effect is quite small. Even for a strain as small as $2\times10^{-5}$, where for the 84-MHz pump there was no parametric contribution for the collinear case at large $|\gamma|$'s, here there is very little difference between the phase-matched and collinear cases. The difference stems from the larger $|\eta|$'s for the higher pump frequency, since the $\Delta k$'s for the two frequencies are comparable at large $|\gamma|$. At small $|\gamma|$'s, however, the very large $\Delta k$ for the 1-GHz pump results in the phase-matched case being strongly favored. For a strain of $2\times10^{-5}$ in the range $-1 \le \gamma \le 1$ the pump makes no contribution to collinear gain, while

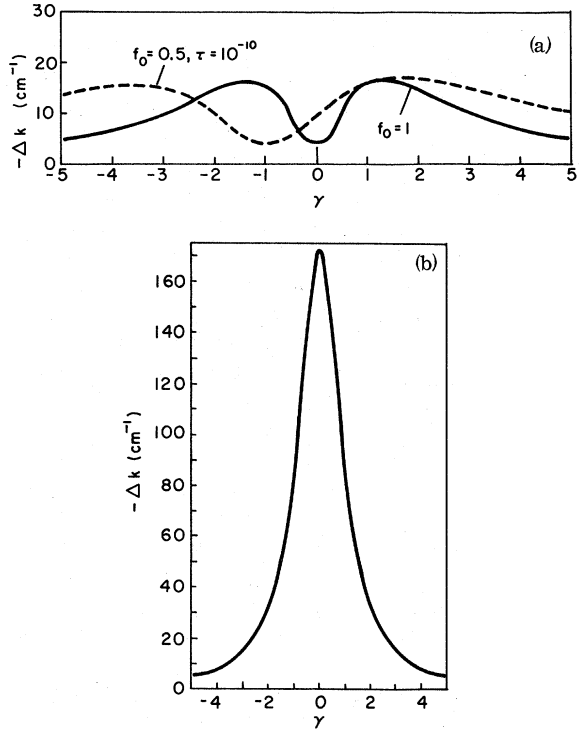


FIG. 9. (a) $\Delta k$ vs $\gamma$ for an 84-MHz pump, collinear 42-MHz signal and idler, with (dashed line) and without (solid line) trapping. $\omega_c = 5\times10^8$/sec. (b) $\Delta k$ vs $\gamma$ for a 990-MHz signal and idler, with $\omega_c = 1.68\times10^9$/sec and no trapping assumed.

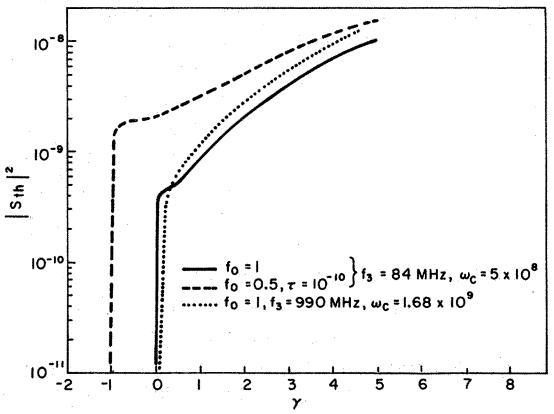


FIG. 10. Square of threshold strain for net amplification of the subharmonic vs $\gamma$ for the cases shown. Phase matching was assumed.

its contribution to phase-matched gain is considerable. Even for a strain of $6\times10^{-5}$ the pump makes no contribution in the range $-0.1 \le \gamma \le 0.1$, and the collinear gain is well below the phase matched until $|\gamma| > 1$.

### D. Threshold Pump Strains

The plots of Figs. 6–8 give a little information on the pump strain required to make parametric gain overcome lattice and linear electronic losses. In this section we examine more systematically how the threshold pump strain required for net gain varies with some of the parameters. In Fig. 10 there is plotted the square of threshold strain, $s_{th}$, vs $\gamma$ for net amplification of the subharmonic, under phase-matched conditions, by pumps of 84 and 990 MHz. The decrease in threshold with decreasing $\gamma$, which has been observed experimentally,[21] is, of course, due to the decrease in $\alpha_e$. It is noteworthy that threshold strains are not much different for 84 MHz without trapping and 990 MHz. The larger parametric gains possible with the higher pump frequency are essentially offset by larger losses, mainly electronic in origin. The flattening in the threshold strain observed for the 84-MHz cases just before $s_{th}$ drops to zero is due to the dip in $|\eta|$ or $|\eta^t|$, respectively, around $|\gamma| = 0$. The thresholds for other values of $\omega\tau$, but $f_0$ still 0.5 and $f_3$ still 84 MHz, usually lie between the dashed and solid curves. For some cases, however, notably for $\tau = 10^{-7}$ and $10^{-8}$, at large $\gamma$'s the threshold strains are found to lie below the solid curve. This is the result of $|\eta^t|$ being greater than $|\eta|$ at large $\gamma$'s [see Fig. 5(a)].

Finally, in Fig. 11 we show the variation of threshold strain with signal frequency for various pump frequencies and $\gamma$'s. For the lower two pump frequencies $s_{th}$ is a minimum at the subharmonic, corresponding to $|\eta|$ being a maximum there. At the highest pump frequency the minimum threshold strain is well away from the subharmonic. This occurs because $|\eta|$ does not peak at the subharmonic, the angular frequency of the pump being greater than $6\omega_{mg}$ for this case. For the cases shown in Fig. 11, $s_{th}$ varies slowly with frequency. One would therefore expect a wide band of frequencies to be amplified. This is commonly observed, although not invariably the case.

## V. UPCONVERSION

### A. Nondegenerate Case

In this section we consider the case in which there are initially two waves, with frequencies $\omega_1$ and $\omega_2$ and wave vectors $\vec{k}_1$ and $\vec{k}_2$, respectively, which combine to form a third wave with frequency $\omega_3 = \omega_1 + \omega_2$. Because of conservation of crystal momentum, the wave generated in this way will have wave vector $\vec{k}_1 + \vec{k}_2$, the direction of which will be taken as the $x$ axis. It will be assumed in this section that the wave vector $\vec{k}_3$ of a freely propagating wave with frequency $\omega_3$ is not equal to $\vec{k}_1 + \vec{k}_2$. Also, the dc field $E_0$ will be taken in a direction other than $x$, such that it makes an angle $\theta_m$ with the wave vector $\vec{k}_m$.

By the use of Eq. (2.13) we find that the second-

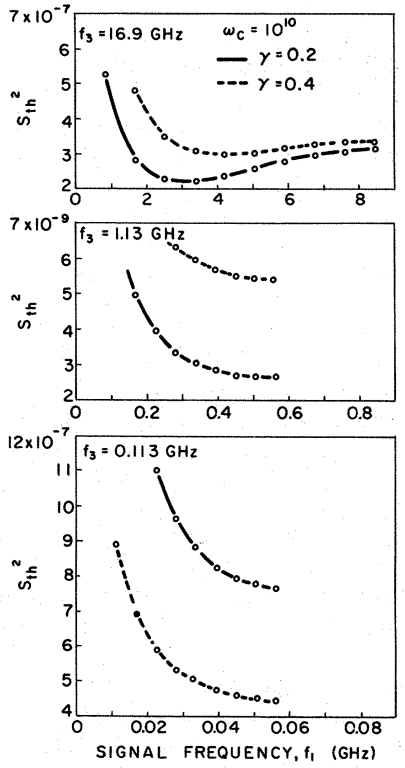


FIG. 11. $S_{th}^2$ vs signal frequency for various pump frequencies and $\gamma$ values. $\omega_c = 10^{10}$/sec and phase matching was assumed for all cases.

order field $\hat{E}_3^{(2)}$ is given by the expression of (2.15b) multiplied by $e^{-i|\Delta\vec{k}|x}$, where $\Delta\vec{k}=\vec{k}_3-\vec{k}_2-\vec{k}_1$ and is parallel to $x$. Also we have

$$\gamma_m = 1 \pm \mu E_0 \cos\theta_m / v_s \, .$$

The set of Eqs. (3.9) is still valid for this case. If we limit ourselves to small enough $x$ so that the amplitude at $\omega_3$ is still small, we may, in this case, neglect the terms involving $\hat{E}_1^{(2)}$ and $\hat{E}_2^{(2)}$. Equations (3.9a) and (3.9b) are then decoupled from each other and from (3.9c) and have simple exponential solutions $\hat{u}_i = \hat{u}_i(0) e^{-\alpha_i x/\cos\theta_i}$ Equations (3.9c) may then be written

$$\frac{d\hat{u}_3}{dx} = -\alpha_3 \hat{u}_3 + \mathcal{A}\hat{S}_1(0)\hat{S}_2(0) e^{-Kx} \, , \tag{5.1}$$

where

$$\mathcal{A} = \frac{ie^3\mu}{4\epsilon^2 c v_s} \frac{\omega_c}{\omega_3} \times \frac{(\gamma_1 + i\omega_1/\omega_D)\cos\theta_1 + (\gamma_2 + i\omega_2/\omega_D)\cos\theta_2}{\Gamma_1\Gamma_2\Gamma_3}$$

for $\omega_1 \neq \omega_2$ (5.2)

and

$$K = (\alpha_1/\cos\theta_1) + (\alpha_2/\cos\theta_2) + i\Delta k \, . \tag{5.3}$$

The differential equation (5.1) is easily solved. With the boundary condition $\hat{u}_3(0)=0$ the solution is

$$\hat{u}_3 = \frac{\mathcal{A}\hat{S}_1(0)\hat{S}_2(0)}{\alpha_3 - K} \left[ e^{-Kx} - e^{-\alpha_3 x} \right]. \tag{5.4}$$

It is more informative to look at the complete expression for the propagating wave, $u_3 = \hat{u}_3 \exp[i(k_3 x - \omega_3 t)]$. With (5.4) this becomes

$$u_3 = \frac{\mathcal{A}\hat{S}_1(0)\hat{S}_2(0)}{\alpha_3 - (\alpha_1' + \alpha_2' + i\Delta k)} \times \left[ e^{-(\alpha_1' + \alpha_2')x} e^{i(|\vec{k}_1 + \vec{k}_2|x - \omega_3 t)} - e^{-\alpha_3 x} e^{i(k_3 x - \omega_3 t)} \right], \tag{5.5}$$

where $\alpha_1' \equiv \alpha_1/\cos\theta_1$ and $\alpha_2' \equiv \alpha_2/\cos\theta_2$. The first of the two terms in the square brackets represents the "forced" wave, with attenuation (or gain) the combined attenuation (or gain) of $\hat{u}_1$ and $\hat{u}_2$, whereas the second represents the free wave with the attenuation (or gain) characteristic of $\omega_3$. The situation is entirely similar to that considered by Mauro and Wang[22] for collinear waves, and (5.5) reduces to their expression when $\theta_1=\theta_2=\alpha_1=\alpha_2=0$. [Also their factor $(k_1+k_2)/k_3$ must be replaced by unity, as we have done earlier.] As pointed out by them and discussed in Sec. III for the downconversion case, if the $\alpha_e$'s are nonvanishing the lack of phase matching will superimpose a ripple on an exponentially varying amplitude. For small $\alpha x$ the ripple will be quite large, of course.

### B. Second-Harmonic Generation

Since we shall be dealing extensively in Sec. VI with both second-harmonic generation and subharmonic generation it is convenient to introduce the abbreviations SecHG and SubHG, respectively. For SecHG a treatment similar to that of the preceding section,[23] with some additional manipulation, leads to

$$|\hat{s}_{2\omega}| = G(2\omega)\,|\hat{s}_\omega(0)|^2 [(e^{-2\alpha_\omega x} - e^{-\alpha_{2\omega} x})^2 \cos^2(\tfrac{1}{2}\Delta k x) + (e^{-2\alpha_\omega x} + e^{-\alpha_{2\omega} x})^2 \sin^2(\tfrac{1}{2}\Delta k x)]^{1/2}, \tag{5.6}$$

where

$$G(2\omega) = |\mathcal{A}|\, k_{2\omega}/2[(\alpha_{2\omega} - 2\alpha_\omega)^2 + (\Delta k)^2]^{1/2} \, . \tag{5.7}$$

Expression (5.6) is valid within the linear, or small bunching, regime. At large amplitudes there is of course an additional contribution to SecHG from the distortion of the wave resulting from the inability of the bunching to follow.[24] The presence of trapping also affects SecHG [25] but that will not be discussed here.

The coefficient $G(2\omega)$ is of primary importance in determining how the efficiency of SecHG varies with frequency, $\gamma$, $\omega_c$, etc. Although $G(2\omega)$ is a more complicated function than $|\eta|$, for $\gamma=0$ it is possible to make some simple analytic deductions if the lattice losses are neglected. This is a good approximation in most of the range of our interest since they are generally small compared to $\Delta k$ or $\alpha_e$ or both. It is found that, for $\gamma=0$, $G(2\omega)$ peaks at $\omega=\omega_{mg}$, having the peak value

$$G_m = (e\mu/6\epsilon v_s)\,(\omega_c/\omega_{mg} + \omega_{mg}/\omega_D)^{-1} \quad (\gamma=0). \tag{5.8}$$

For shear waves in the basal plane of CdS the quantity $e\mu/6\epsilon v_s$ is $9\times10^3$. It is seen from (5.8) that $G_m$ decreases monotonically with increasing $\omega_c$, or more precisely with increasing $n_0$. For $\gamma\neq0$ it can be deduced from (5.7) and (5.2) that there will be little change in $G(2\omega)$ when $(\omega^2/\omega_D^2) \gg \gamma^2$. These features can be seen in the plots of $G(2\omega)$ vs $\omega$ shown in Fig. 12. For each $\omega_c$ the maximum in $G(2\omega)$ does indeed occur at $\omega_{mg}$ for $\gamma=0$, as predicted. For the larger $\omega_c$, where $\omega_{mg}/\omega_D > 1$, the peak value is the same for $\gamma=-1$ as for $\gamma=0$. For small $\omega^2/\omega_D^2$ the $\gamma$ dependence comes mainly from the factor $(\gamma^2 + \omega^2/\omega_D^2)^{1/2}$ in the numerator of $|\mathcal{A}|$. Thus for small $\omega$ the curves for $\gamma=-1$ lie above those for $\gamma=0$. In the various features just described $G(2\omega)$ is quite similar to $|\eta|$ for the same

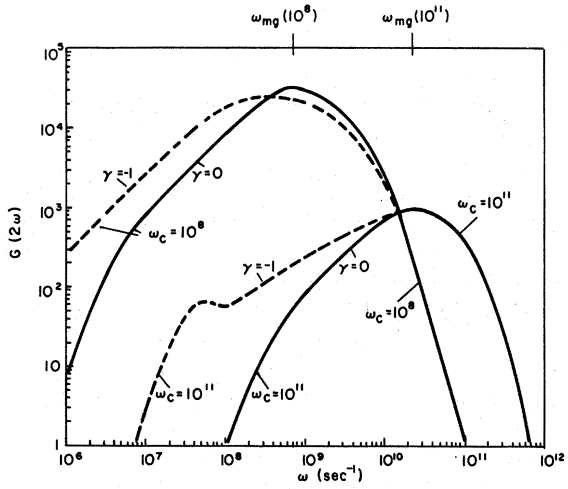


FIG. 12. $G(2\omega)$, defined by Eq. (5.7), vs $\omega$ for different values of $\omega_c$ and $\gamma$, for shear waves in the basal plane of CdS.

$\omega_c$'s and $\gamma$'s (compare Fig. 12 with Fig. 4). The major difference is that $G$ falls off much less rapidly with frequency on the low-frequency side. (The fact that $G$ falls off more rapidly for high frequencies than it does for low ones is due to the steep increase with $\omega$ of lattice loss.) The less rapid variation at low frequencies is due to the presence of the factor in the denominator of $G$ involving $\Delta k$. The factor $\frac{1}{2}|\mathcal{A}|_{k_{2\omega}}$ is very similar to $|\eta|$ and, like $|\eta|$, peaks around $\omega_{mg}$. However, $\Delta k$ also peaks around $\omega_{mg}$, with the consequence that the steepness of growth of $G(2\omega)$ is cut down as $\omega$ grows toward $\omega_{mg}$.

Before leaving this section, we note that for SecHG a complete solution of the Eqs. (3.9) is available, i.e., a solution whose validity is not limited to the region of small depletion of the fundamental, for the case $\gamma=0$, $\Delta k=0$ and lattice loss is small enough to be neglected. For this case the coupled equations may be written

$$\frac{d\hat{u}_{2\omega}}{dx} = i\mathcal{A}_0 k_\omega^2 \hat{u}_\omega^2 , \tag{5.9a}$$

$$\frac{d\hat{u}_{\omega}}{dx} = 4i\mathcal{A}_0 k_\omega^2 \hat{u}_\omega^* \hat{u}_{2\omega} , \tag{5.9b}$$

where $\mathcal{A}_0 = i(\frac{1}{2}\mathcal{A})|_{\gamma=0}$, a real quantity. Assume now that $\hat{u}_\omega = \rho_\omega$, $\hat{u}_{2\omega} = i\rho_{2\omega}$, where the $\rho$'s are real.[26] For the boundary condition at $x=0$ that $\rho_{2\omega}=0$ and $\rho_\omega = \rho_\omega(0)$, conservation of energy requires that

$$\rho_\omega^2 = \rho_\omega^2(0) - 4\rho_{2\omega}^2 . \tag{5.10}$$

When the $\hat{u}$'s are replaced by $\rho$'s in Eqs. (5.9), the condition (5.10) may be used to eliminate $\rho_\omega$ from (5.9a), making integration of that equation straightforward. Similarly, (5.10) may be used to eliminate $\rho_{2\omega}$ from (5.9b) so that the equation may be integrated. For the boundary condition we have chosen, the resulting solution is

$$|\hat{S}_{2\omega}| = |\hat{S}_\omega(0)|\tanh[2\mathcal{A}_0 k_\omega |\hat{S}_\omega(0)| x] , \tag{5.11a}$$

$$|\hat{S}_{\omega}| = |\hat{S}_\omega(0)|\operatorname{sech}[2\mathcal{A}_0 k_\omega |\hat{S}_\omega(0)| x] . \tag{5.11b}$$

It is readily seen that, for small $x$, (5.11a) goes over to the result obtained from (5.6) for small $x$ when $\Delta k$ and the $\alpha$'s are set equal to zero.

## VI. COMPARISON WITH EXPERIMENT

There are considerable data to which the foregoing theory may be applied, qualitatively at least. The most clearcut are those in which a pump was introduced from outside and the resulting amplification studied. We shall discuss these in Sec. VI A. In other experiments SubHG was observed even though a pump was not introduced from the outside. Data on moving domains, obtained by many workers, indicate that a great deal of mixing, both downconversion and upconversion, is taking place there. We shall discuss these phenomena in Sec. VI B.

### A. Parametric Experiments

The first clear evidence for parametric amplification through acoustoelectric coupling of different acoustic waves was obtained for bulk shear waves propagating in the basal plane of CdS. A pump of 1 GHz was shown to amplify acoustic thermal noise of 0.5 GHz.[21] This work demonstrated also net gains for $v_d < v_s$, the threshold pump strain required for net gain increasing with decreasing $v_d$, in agreement with the trend shown in Fig. 10. Further experiments demonstrating parametric amplification due to this mechanism, in which a pump and in some cases also a signal were introduced from outside, are discussed in Refs. 18, 27, and 28. The data most susceptible to quantitative treatment are presented in Fig. 13. They were taken on shear waves in the basal plane of a CdS sample with $\rho = 715\ \Omega$ cm, corresponding to $\omega_c = 1.68\times10^9$/sec. It will be recognized that extensive numerical results were presented for this case in Sec. IV.

Before going into a detailed discussion of data in Fig. 13 it is worthwhile to review some of the relevant experimental details. The pump power was introduced into the sample at $x \simeq 0$[29] and amplified by a dc field of magnitude such that $-0.2 \leq \gamma \leq -0.1$. At these $\gamma$ values the noise background and acoustoelectric current were still very small. It is reasonable therefore to assume a uniform field $E_0$, apart from 10–20% variations due to sample inhomogeneity. Without the pump on, no power was detected at the subharmonic frequency (nor any other) anywhere in the sample. This is par-

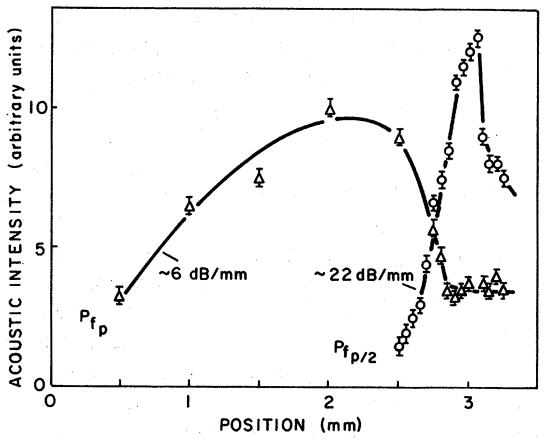


FIG. 13. Power at the pump frequency, $p_{f_p}$, and at the subharmonic, $p_{f_{p/2}}$, vs distance for a phase-matched case in CdS with $\omega_c = 1.68 \times 10^9$/sec (taken from Zemon and Zucker, Ref. 28).

ticularly significant since the frequency of maximum gain, $\omega_{mg}/2\pi$, is 0.46 GHz, very close to the subharmonic. The gain value for the pump stated in the figure, 6 dB/mm, corresponding to 6.9Np/cm, is derived from the first two measured points. With the pump on, the subharmonic first became visible (by Brillouin scattering) at about 2.5 mm. The subharmonic was not the only frequency seen. A wide band of frequencies was amplified. The amplitudes were greatest in the neighborhood of the subharmonic, in agreement with the foregoing theory. The intensity of the subharmonic was observed to increase exponentially at a rate of 22 dB/mm, corresponding to 25.4 Np/cm, between about 2.5 and 2.8 mm. Between 2.8 and 3 mm the increase is less steep, presumably because the pump intensity has gotten much smaller. Beyond 3 mm the decrease in $\frac{1}{2}f_p$ is probably due to the generation of $\frac{1}{4}f_p$. This surmise could not be verified experimentally, however, due to the difficulties in detecting such a low frequency.[19] The maximum pump strain, at 2 mm, was estimated to be $1 \times 10^{-6}$.[19] This value was calculated[30] from the measured amount of light scattered by the pump and an approximate value for the photoelastic constant $p_{44}$.[31] The pump and each of the signals within the amplified band were found experimentally to propagate at the angles required for phase matching according to linear theory. This latter fact, as well as the estimate of the pump strain, indicates that the strains are small enough so that the principal approximations made in the development of Secs. II, III, and V should be good.

Since both linear and parametric gain are present, the first task of theory is to separate the two. To do this we assume that the pump loss due to parametric amplification is negligible for $x < 1$ mm. There is lattice loss, however, of 6.1Np/cm, according to Table I, giving a linear electronic gain for the pump of 13 Np/cm. With the use of Eq. (3.6) (and neglect of trapping, usually unimportant at these frequencies) and the parameters of Table I, this leads to $\gamma = -0.18$. Since acoustoelectric current was still negligible in the presence of the strong pump, we assume this $\gamma$ value is valid also where the signal is being strongly amplified. Correcting the observed net gain of the signal for lattice loss, 2.2 Np/cm, we find that the sum of linear and parametric gain for the signal is 27.6 Np/cm. For $\gamma = -0.18$ the linear gain at this frequency is 21.4 Np/cm, leaving only 6.2 Np/cm of parametric origin.

Having separated out the parametric gain, and noted that the growth varies exponentially with distance, we are now able to carry out a comparison with the theory of Sec. III. Since subharmonic and pump were phase matched, if the pump intensity had been constant, by Eq. (3.23), $6.2 = |\eta'||S_3|/\cos\theta$. With $\theta = 6°$ for this case, we may take $\cos\theta = 1$ and use $|\eta|$ instead of $|\eta'|$. For $\gamma = -0.18$, as can be seen from Fig. 5(b) where the parameters match those of the experiment, $|\eta| = 1.45 \times 10^6$, this value not being particularly sensitive to $\gamma$. This leads to $|S_3| = 4.3 \times 10^{-6}$, which must represent some kind of average since the pump strain is not actually constant. This strain is well above the estimate of $1 \times 10^{-6}$ cited earlier for the maximum pump strain. That the strain value had to be well above $1 \times 10^{-6}$ could have been deduced immediately from Fig. 8. For a strain of $2 \times 10^{-6}$ there is, for small $\gamma$, almost no difference between the solid line representing total phase-matched gain and the dotted line representing $-\alpha_e - \alpha_l$. One might be tempted to argue that the strain was actually only $1 \times 10^{-6}$ and the observed gain, after correction for lattice loss, is simply the linear gain $-\alpha_e$. A higher value of $-\alpha_e$ could easily be accounted for by assuming a slightly larger $-\gamma$ in this region. Fortunately, there is another type of argument for the larger strain value that is independent of the magnitude of $\gamma$. Let $l$ denote the distance through which parametric amplification takes place. For large enough $l$ and constant pump strain the ratio of the subharmonic intensity with the pump present to that without a pump is $(e^{|\eta||S_3|l})^2$. If we take the intensity of $\frac{1}{2}f_p$ at $x = l$ in the presence of the pump to be 50 in arbitrary units, then for $\frac{1}{2}f_p$ to have been experimentally unobservable at the same $l$ without a pump it must have been 1 or less in the same units.[19] Thus $e^{2|\eta||S_3|l} > 50$. With $l = 3$ mm this leads to $|\eta||S_3| > 6.5$. In the range $-1 \leq \gamma \leq 0$, $|\eta|$ varies from $2.1 \times 10^6$ to $1.3 \times 10^6$, the former being its maximum value, as shown in Fig. 5(b). For $\gamma$ close to zero, the minimum value of $|S_3|$ is close to $5 \times 10^{-6}$ by this argument. Even for the

peak value of $|\eta|$, $2.1\times10^{6}$, $|S_3|$ would be greater than $3\times10^{-6}$.

Thus it appears that the theory can account, at least qualitatively, for some of the principal experimental observations provided the average strain is $\sim4\times10^{-6}$ or perhaps a little larger. The discrepancy between this and the maximum value of $1\times10^{-6}$ deduced from the scattered light is likely to be due to $p_{44}$. The value used, 0.054, was taken from Dixon.[31] He lists this value as approximate but does not say how large the error might be. However, Maloney and Carleton,[32] who also made measurements of photoelastic constants, claim that $p_{44}$ for CdS is too small to measure.

Parametric theory can also account for the variation with distance of the pump intensity. As shown in Fig. 13, at positions well before those for which $\frac{1}{2}f_p$ is visible there is a considerable flattening of $P_{f_p}$, i.e., it falls considerably below an expontenial increase. It has been suggested that this flattening represents a decrease in $-\alpha_l$ due to a large bunching, produced presumably by large pump amplitude. This type of nonlinearity has been discussed by many workers.[33-37] The suggestion is not plausible, however, because the large amplitude nonlinearity requires strains much larger than $5\times10^{-6}$, i.e., much larger than would be consistent with the experimental data. At $5\times10^{-6}$ the maximum fraction of the carriers that would be bunched for the sample and frequency we are discussing is about 0.1, according to linear theory. Even at $1\times10^{-5}$ it would only be $\sim0.2$. It should be remembered also that the phase-matching angles were in good agreement with linear theory, indicating that the strain was still small enough for the dispersion to follow linear theory.

We can show that the flattening is reasonably attributed to energy loss in parametric amplification. Although for $x<2.5$ mm the amplified frequencies are still too small for any one (more exactly, any small range) to be visible by Brillouin scattering, they occupy a sufficiently wide band so that they represent considerable energy. At the 3-mm position, where $\frac{1}{2}f_p$ has its maximum amplitude, the half-width of the band is 200 MHz, as shown in Fig. 5 of Ref. 28. At smaller values of $x$, where there has been less gain, the half-width must be still larger. We can use this bandwidth to make a crude estimate of the total power in the amplified noise at 2.5 mm where $\frac{1}{2}f_p$ is first visible. The experimental resolution is such[28] that each point represents the intensity in a frequency range of 50 MHz. (Note that for two frequencies differing by 50 MHz the angles at which phase matching occurs differ by less than 1°, the angular resolution of the apparatus.) Thus crudely, with a bandwidth of $4\times50$ MHz the energy represented in the noise will be about four times the value shown in Fig. 13 for $\frac{1}{2}f_p$. Since the bandwidth of the pump is less than 1 MHz, probably about 0.1 MHz, and its angular spread is less than 1°, each experimental point for the pump gives the entire pump intensity. Thus at 2.5 mm, where $P_{f_p}\simeq6P_{f_p/2}$ from Fig. 13, the total intensity in the noise is about $\frac{2}{3}$ of the pump intensity. We conclude that even at the point where $\frac{1}{2}f_p$ is first visible it is reasonable to expect that the pump has already lost a good deal of energy in downconversion. Obviously, this process must have begun before the point where $\frac{1}{2}f_p$ became visible to the Brillouin scattering. At small $x$, where the noise amplitude is small, the energy loss is small and the pump growth does not fall far below the exponential. When the amplitudes become large the rate of pump depletion increases until the pump amplitude actually decreases despite the continued existence of linear gain. To make these ideas more quantitative we have calculated the growth at each signal frequency, starting from the thermal equilibrium value at $x=0$ and assuming all waves collinear and phase matched. Pump depletion was neglected for this part of the calculation and Eq. (3.14) was used for each frequency with $\Delta k=0$. The rate of change with $x$ of the sum of signal and pump energy is equal to the rate at which energy is gained due to linear amplification. With total signal energy known as a function of $x$ from the previous calculation, this condition leads to a linear differential equation that is easily solved to give pump energy vs distance. The shape of the resulting curve was quite similar to that shown in Fig. 13. Indeed, when a pump strain of $4\times10^{-6}$ was used in calculating the downconverted energy the rapid decrease in pump intensity was found to occur at about 3 mm, as shown experimentally.

An important implication of the foregoing discussion is that the theories dealing with large amplitude effects[33-37] of a single wave may be quite limited in their applicability. Under conditions where the rate of loss in parametric amplification and upconversion becomes comparable to the gain rate, the amplitude of the wave may not grow large enough for the predicted effects to be important.[38] As a corollary, the observation of "saturation of the linear gain" at large strain amplitudes in CdS by many workers[39] is likely to have been at least partly due to energy losses in mixing with the noise. This situation should be further investigated, preferably by Brillouin scattering.

Although experiments in which a pump was introduced from the outside have not, to our knowledge, been reported for GaAs, there is considerable evidence for subHG by the acoustoelectric mechanism in that material. That first such evidence, and the only part not involving acoustic domains, was obtained by the observation of current noise under

strong amplification as a function of time.[40] The noise showed several wide peaks, one at $f_{mg}$, others at $\frac{1}{2}f_{mg}$ and $\frac{1}{4}f_{mg}$. As time progressed, the latter two peaks grew while the former did not.

### B. Domains

When traveling acoustic domains were first studied by Brillouin scattering, it was observed that the frequency at which the intensity is a maximum, $f_{mi}$, and that at which the net gain is a maximum decrease as the acoustic intensity increases. The decrease may be by as much as an order of magnitude. The first observations of this effect were made on CdS.[41] They were verified by a good deal of later work, both on CdS and GaAs.[42] Following the evolution of various different frequencies as domain moves, both during and after application of the voltage, many workers have obtained detailed information establishing that downconversion by parametric amplification and upconversion are both going on. Before going into the discussion of a full-blown domain in semiconducting material, we shall find it profitable to do some further calculations for the experimental situation discussed extensively in Sec. V.

#### 1. *Low-Flux Domain*

In the experiments discussed in Sec. VI A, the pump was applied only briefly, for an interval of 0.5 $\mu$sec. What propagated then was a narrow pulse of relatively high-intensity flux, which of course constitutes a domain. Compared to the usual mature domain, however, it could be called a low-flux domain. It is a simpler one to study than the usual one since, as we saw, the frequency spectrum was limited, the acoustic intensities remained reasonably within the realm of linear theory, and the acoustoelectric current was small enough so that $v_d \simeq \mu E_0$. (The experiments were, in fact, intended to set up a domain that would be simpler to study.)

Consider the parametric amplification that would be caused by $\frac{1}{2}f_p$, 495 MHz, acting as a pump for its subharmonic. We find $|\eta|$ for this case to be smaller by a factor of 1.7 than the value calculated earlier for 990 MHz pumping its subharmonic. In addition, $\frac{1}{2}f_p$ is a less coherent pump than $f_p$ was. Nevertheless, since the magnitude of $\frac{1}{2}f_p$ gets somewhat larger than that of $f_p$, as shown in Fig. 13, it is reasonable that $\frac{1}{2}f_p$ will generate $\frac{1}{4}f_p$. As noted earlier, this could not be verified in these experiments. However, generation of $\frac{1}{4}f_p$ from $\frac{1}{2}f_p$ was seen in a similar sample, for the same pump, when application of a somewhat greater voltage led to generation of $\frac{1}{4}f_p$ closer to the center of the sample, a more convenient position for viewing it. Thus, the original $f_{mi}$ would almost certainly have been downshifted by a factor of 4. The downshifting would not, however, continue indefinitely. First, $\frac{1}{4}f_p$ will not grow as large as $\frac{1}{2}f_p$ at its peak because the linear gain at this frequency is smaller, down to about 14 Np/cm. Then, $|\eta|$ for generating $\frac{1}{8}f_p$ from $\frac{1}{4}f_p$ is down by almost a factor of 4 from that for generating $\frac{1}{4}f_p$ from $\frac{1}{2}f_p$. In addition, $\frac{1}{4}f_p$ will be still less coherent than $\frac{1}{2}f_p$. Thus the generation of $\frac{1}{8}f_p$ from $\frac{1}{4}f_p$ will be considerably less than that of $\frac{1}{4}f_p$ from $\frac{1}{2}f_p$. Finally, at $\frac{1}{8}f_p$ further subHG should be negligible because of a combination of still smaller $|\alpha_e|$ and $|\eta|$, the latter being reduced by a further factor of 7 (thus down by a factor of 42 from $|\eta|$, for the 990-MHz pump) and still less coherence.

Consider now the situation for SecHG and upconversion for this simple domain. Because lattice loss grows rapidly with frequency, under the conditions of the experiment $\alpha_l > |\alpha_e|$ for both the second harmonic of $f_p$, 1980 MHz, and the sum $f_p + \frac{1}{2}f_p$, 1485 MHz. As a consequence only the forced wave is found at large $x$. According to (5.6) then, the coefficient of $G(2\omega_p)$ at large $x$ is

$$|\hat{S}_{\omega_p}(0)|^2 e^{-2\alpha_{\omega}x} \equiv |\hat{S}_{\omega_x}(x)|^2 .$$

The quantity $\frac{1}{2}|\mathcal{J}|k_{2\omega_p}$ is $9\times10^5$/cm and $\Delta k$ is $-148$ cm much larger than $\alpha_{2\omega_p} - 2\alpha_{\omega_p}$. Thus, even if the maximum value of $|\hat{S}_{\omega_p}(x)|$ were $10^{-5}$, the intensity at $2f_p$ would be insufficient to be seen. The situation is somewhat more favorable for observing the sum of pump and subharmonic frequencies since $|\mathcal{A}|k_{3\omega_p/2} \simeq 2\times10^6$ and, although $\Delta k$ is somewhat larger than for SecHG, it is not a great deal so. It is difficult to estimate the maximum value of the product of the strains at $f_p$ and $\frac{1}{2}f_p$. It should be less than $10^{-10}$, however, which would not be enough to make the sum frequency visible. These results are consistent with the experimental results. Neither $2f_p$ nor $f_p + \frac{1}{2}f_p$ was seen until the applied voltage was increased, increasing the gain and therefore the strain amplitudes. Not surprisingly, in view of the above discussion, when the voltage was increased, $f_p + \frac{1}{2}f_p$ appeared before $2f_p$.[19]

Consider now the situation for upconversion from $\frac{1}{2}f_p$ and lower frequencies. We find that $G(2\omega)$ does not change much with frequency in the range $f_p - \frac{1}{8}f_p$. It increases somewhat as the frequency is lowered from $f_p$ to $\frac{1}{2}f_p$, where it peaks since, as noted earlier, $\frac{1}{2}f_p$ happens to be close to $f_{mg}$. At $\frac{1}{8}f_p$ it is within 10% of its value at $f_p$. Thus, if the applied voltage had been increased sufficiently to see SecHG at $f_p$, one would expect to see it for fundamental at $\frac{1}{2}f_p$, $\frac{1}{4}f_p$, $\frac{1}{8}f_p$, and still lower frequencies, forgetting about possible experimental difficulties. This is in constrast to the situation with subHG.

#### 2. *Applicability of Second-Order Theory*

The usual full-blown domain differs from the simple one we have just been studying in two im-

portant ways. There is no coherent large amplitude pump and the voltage is not kept low. When the high voltage is applied there is high gain in the resulting high-field regions. For simplicity let us assume that there is one such near the cathode, a frequent occurrence in CdS samples. In this region many different modes, originating in the noise, grow rapidly in amplitude. After some distance of travel, short enough so that amplitudes are still in the linear range, it is expected that the energy be spread out over a wide range of frequencies and some range of propagation directions. As the waves (which by now may be considered to constitute a domain) progress and amplitudes continue to grow, the point will be reached at which appreciable mixing can occur. To discuss the mixing, we may consider that the waves in a small range of frequencies $\Delta f$ around an arbitrarily chosen frequency $f_0$, with a small range of propagation angles, act as a single coherent wave with frequency $f_0$. The range $\Delta f$ must be taken small enough so that the coherence distance (which may be defined arbitrarily as the distance in which the phase difference between $f_0 + \frac{1}{2}\Delta f$ and $f_0 - \frac{1}{2}\Delta f$ becomes $\frac{1}{2}\pi$) is of the order of a millimeter. This is necessary for obtaining observable effects on the scale we have been discussing. For shear waves in CdS $\Delta f \simeq 0.5$ MHz. This is somewhat larger than the upper limit for the bandwidth estimated for the 1-GHz pump we discussed earlier. It is to be expected that these partially coherent waves participate in all of the mixing processes that have been discussed earlier.

It is interesting to compare the mixing in the situation we have been discussing, which might be called the random case, with that in the situation discussed earlier in which there is only one coherent large-amplitude wave, produced by introduction of a coherent pump from outside. With the intensity of the one wave comparable to that of the largest waves in the random case, it would be reasonable to expect a lot more mixing in the latter case. Primarily this would be so because there are so many more large coherent waves in the latter case. In addition, interaction of different waves is also furthered by the randomness in direction of the large-amplitude waves, which would cause them to overlap more different waves. One can go further and show that the rate of energy loss due to mixing should be larger for a coherent wave in the random case than for the single coherent wave in the other case, when the two have the same frequency and intensity. This is true because of the greater number of large-amplitude waves available as mixing partners in the random case. Both the rate of loss in downconversion [as can be deduced from Eqs. (3.9c) and (2.15b)] and in upconversion [as can be deduced from Eq. (5.4) or alternatively from (3.9) and (2.15)] increase as the amplitude of the other waves participating increases. As a corollary, amplitudes are less likely to grow large enough for large bunching effects to occur in the random case.

It appears that the effects we have been discussing are illustrated in an experiment[27] in which a coherent pump with frequency a little higher than $f_{mg}$ was introduced from outside into a ZnO sample with $v_d$ sufficiently greater than $v_s$ to cause current saturation. The sample was inhomogeneous and showed net acoustic gain only in a short region, about 1 mm long, near the cathode. Before the introduction of the pump this region of the sample showed (by Brillouin scattering) a continuous acoustic noise spectrum peaked at about 2.2 GHz. After introduction of the pump, which had a frequency of 2.85 GHz, there were narrow peaks at 2.85 GHz and at its subharmonic, and a minimum at 2.2 GHz. Measurements did not extend far enough to show whether there were additional peaks at $\frac{1}{4}f_p$ or $f_p + \frac{1}{2}f_p$. Existence of strong peaks at these other frequencies is, however, unlikely, in the latter case because of the large lattice loss at this frequency, in the former because of the short length of gain path. Significantly, the total amount of acoustic flux was considerably reduced, by about a factor of 8 in the range of measurement, in the presence of the pump. (Small peaks outside the range of measurement would not affect this materially.) This suggests that the amplitude of the pump did become large enough to cause large bunching. The large bunching would result in decreased gain, as described by the large-amplitude theories,[33–37] and the total flux would not grow as large as when all was random. Some contribution to the decrease in flux might also have come from the mixing of $f_p$ and $\frac{1}{2}f_p$, which as indicated earlier, would give a strongly absorbed sum frequency. This is the nonlinear loss mechanism suggested earlier by Hutson.[43] This mechanism is not expected to be predominant, however, since for the frequencies concerned downconversion should be stronger than upconversion.

Because of the randomness and basic lack of coherence, and the energy losses in upconversion and downconversion, we feel it is reasonable that, although the total flux in the domain grows very large, the flux in what could be considered a single coherent wave remains small enough so that second-order theory is more or less applicable. Even so, the assumption of small bunching must certainly be violated in the domain at many points in time and space due to overlapping of waves. This will occur in a random way, however, rather than in the systematic way it occurs in a single coherent large-amplitude wave and should therefore have much less effect. In what follows we shall apply the second-order theories and show that they do provide additional insight into what is occurring in

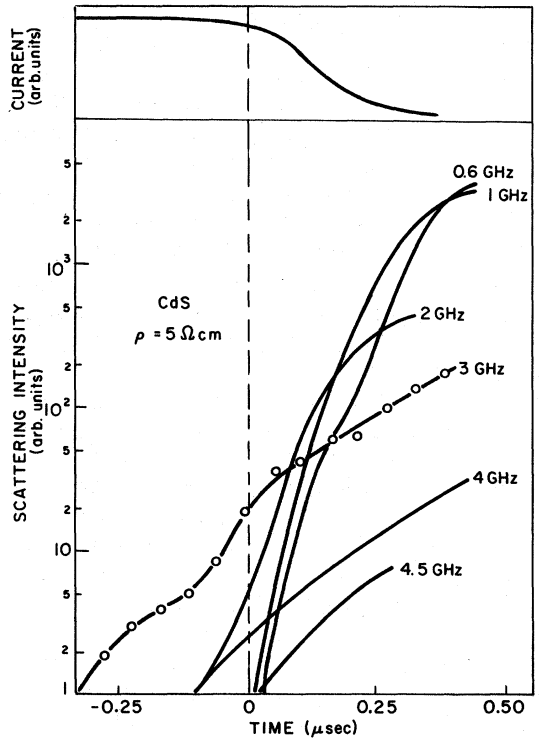


FIG. 14. Current and flux at different frequencies vs time for a traveling domain in a semiconducting CdS sample. The time 0 marks the onset of the deviation in current from the Ohmic value. Measuring points are drawn only for 3 GHz (taken from Wettling and Bruun, Ref. 44).

the fullblown domains.

### 3. *High-Flux Domain—Early Stages*

The type of domain we will now consider is one developed on application of high voltage to a typical semiconducting sample of CdS ($\omega_c \simeq 10^{11}$/sec) or GaAs ($\omega_c \simeq 10^{12}$/sec). With such large $\omega_c$ values $f_{mg}$ is high enough so that corrections for lattice attenuation are not negligible. It is therefore convenient to use instead $f_{mng}$, the frequency of maximum net gain, which is somewhat lower than $f_{mg}$ because of lattice attenuation. The evolution of the frequency spectrum of domains in such samples has been carefully studied by Brillouin scattering, for a number of CdS and GaAs samples in which, coincidentally, $f_{mng} \simeq 3$ GHz. Although these studies were carried out by several different groups,[44–50] many of the results are so similar as to be almost interchangeable. In Fig. 14 we show some typical results, obtained on CdS.[44] Initially, i.e., for times short enough after application of the voltage that there is no current drop, growth was found to follow linear theory. It was very rapid, because of the large value of $|\gamma|$, for a small range of frequencies around $f_{mng}$. After these frequencies had grown to a considerable amplitude (in GaAs Spears[45] found this to be the point at which energy density had reached $10^8$ times thermal) their rate of growth decreased. At this state, lower frequencies, represented by 2 GHz in Fig. 14, began to appear. The rate of growth at these lower frequencies was much greater than predicted by linear theory, as is evidenced by the fact that the 2-GHz curve has a steeper slope than the initial slope for $f_{mng}$, 3 GHz. In the usual GaAs sample,[45] and occasionally for CdS,[46] the spectrum at this stage showed a peak at $f_{mng}/2$. As has already been pointed out by many authors,[28, 44, 45] the steeper growth at lower frequencies and the appearance of the subharmonic are clear evidence for downshifting by parametric amplification rather than large bunching effects. In addition, Spears also found in GaAs that the angular distribution at this stage showed two peaks at the subharmonic frequency 4° apart, as expected for phase matching according to the linear dispersion.[45] Thus, what is going on at this early stage in the high-flux domain is, now surprisingly, quite similar to what was observed in the low-flux domain.[28] Instead of an essentially monochromatic pump, however, there is a group of partially coherent pump frequencies, each one presumably producing a range of frequencies around its subharmonic. Another difference from the simple domain is that pump depletion is not seen because the linear gain is so much greater at the higher voltages. It is the existence of the large linear gain plus the fact that the initial pumping takes place over a relatively wide range of frequencies that tends to obscure the peak in the spectrum at the subharmonic. This peak is more likely to be visible in GaAs than in CdS because the former has a greater value for the ratio $|\eta|/|\alpha_e|$.[28]

### 4. *High-Flux Domain—Later Stages*

At the stage we have been discussing the current had just begun to fall. As the current falls further, still lower frequencies, represented by 0.6 and 1 GHz in Fig. 14, are observed. Again, these grow more rapidly than predicted by linear theory and by the time current saturation is reached have much higher intensities than the higher frequencies. In the range where the current is at or close to saturation, quantitative comparison with theory becomes much more speculative. One question that has been much discussed in the literature is that of the value of $\gamma$, i.e., whether one should use $\gamma = 1 - \mu E/v_s$ or $\gamma = 1 - v_d/v_s$. It has been established recently that the gain is not correlated with the electric field value in the domain,[44, 45, 47] but is reasonably well represented by using $\gamma = 1 - v_d/v_s$ in the first-order theory. It should therefore be meaningful to compare experimental results in the saturation or near-saturation range with our theoretical predictions

using $\gamma$ in the range 0 to $-1$, more specifically close to 0. Fortunately, as has been shown in Sec. IV, the results of the second-order theory are, for large frequencies, insensitive to the magnitude of $\gamma$ in this range. We can get approximate values of $|\eta|$ for subharmonic generation in the sample we are discussing by using the plots of Fig. 4 for $\omega_c = 10^{11}$/sec. These plots are made for $f_{mng}$ slightly greater than 3 GHz, but can be used with little error by taking the value of $|\eta|$ for 3 GHz as that given by the plot for $f_{mg}$, the value for 1.5 GHz at that on the plot for $\frac{1}{2}f_{mg}$, etc. In this way we find that for a 3-GHz pump $|\eta| \simeq 3\times10^5$ while for pumping by $f_{mng}/2.5$ $|\eta| \simeq 3\times10^4$. Thus $|\eta|$ for SubHG by 1.2 GHz is about a factor of 10 smaller than $|\eta|$ for SubHG by 3 GHz. This is similar to the situation discussed earlier for the low-flux domain. In contrast to that situation, however, the strain at the lower frequency is undoubtedly considerably higher. Although data for 1.2 GHz are not given in Fig. 14 it is expected they will be quite similar to those for 1 GHz. For pumping by 0.6 GHz, $\frac{1}{5}f_{mng}$, $|\eta|$ is down to about $2\times10^3$, while for pumping by 0.3 GHz, $|\eta|$ is down by more than another order of magnitude. Data for 0.3 and 0.2 GHz were obtained by Zucker and Zemon[48] on a similar CdS sample. They find the intensities at these low frequencies grow to a level comparable to that at 0.6 GHz. With such a small value of $|\eta|$ as is found at 0.3 GHz, however, further downconversion by this mechanism would no longer be substantial. This appears to be in good agreement with the fact that downconversion of $f_{mi}$ by about a factor of 10 is the maximum that has been reported.

Now consider upconversion. In the low-flux domain discussed earlier the regeneration of $f_p$ from $\frac{1}{2}f_p$ was observed.[19] The observation was possible there because of the partial spatial separation of the two frequencies. In the high-flux domains now under discussion, however, it would not be possible to separate SecHG from the other processes, with the possible exception of the second harmonic of 3 GHz. Lattice loss is so high, however, at 6 GHz that it is not likely to be observed. SecHG must, nevertheless, be considerable in the domains now under discussion. According to Fig. 12, for $\omega_c = 10^{11}$/sec, when the frequency decreases from $f_{mg}$ to $\frac{1}{5}f_{mg}$ there is a decrease in $G(2\omega)$ by only a factor of 2. In the calculations for this figure $\Delta k$ was taken to have the value given by linear theory. Under the high-flux conditions in the domain, $\Delta k$ is likely to be smaller, in which case $G(2\omega)$ would be larger everywhere. The ratio between $G(2\omega)$ at 3 and 0.6 GHz would then be larger than 2, probably, but not a great deal so. The decrease in $\Delta k$ would also decrease interference effects due to lack of phase matching but, as noted earlier, this is not a major effect in the presence of sizable linear gain. We conclude then that, at the time of current saturation, since $|\hat{S}(\omega)|^2$ increases by more than a factor of 20 as the frequency decreases from 3 to 0.6 GHz, according to the data of Fig. 14, SecHG must be considerably stronger at the lower frequencies.

Nondegenerate upconversion, or sum frequency generation, should, according to the theory of Sec. V, be of comparable importance to SecHG. As noted in the discussion of the simple domain, $f_p + \frac{1}{2}f_p$ appeared more strongly than $2f_p$ when the voltage was increased. Wettling and Bruun[44] speculate that part of the 4.5-GHz intensity seen in Fig. 14 may be due to sum frequency generation. Their speculation is based on the late appearance of this frequency and the fact that its gain is somewhat greater than expected from linear theory. For frequencies below 3 or 4 GHz the Brillouin scattering technique cannot generally separate the contributions of downconversion and upconversion. A technique with greater resolving power is that of observing the microwave emission that occurs when the domain arrives at the anode.[49] This emission is believed to be due to electromechanical conversion of the acoustic flux at the anode surface. Observed in the microwave emission, and therefore presumably existing in the domain, are peaks corresponding to $f_{mng}$, $\frac{1}{2}f_{mng}$, $\frac{1}{4}f_{mng}$, $\frac{1}{8}f_{mng}$; sum frequencies of all these; and second harmonics of the sum frequencies.[49]

The foregoing discussion suggests the following picture of the mixing in the domain at the time when $f_{mi}$ has been downshifted from 3 to about 0.6 GHz, i.e., at a time close to current saturation and to the end of the data in Fig. 14. At 3 GHz there is some gain due to the drifting electrons, i.e., linear gain, since $\gamma$ is not equal to 0, and possibly some gain by downconversion from higher frequencies. On the other hand, there is loss in downconversion and presumably smaller loss in upconversion. The fact that 3 GHz is still growing indicates that the linear gain more than makes up for the losses. At 0.6 GHz linear gain is expected to be small, so gain by downconversion must be large enough to somewhat more than balance losses due to upconversion and further downconversion.

### 5. *Effects on Removal of Voltage*

The picture just described appears to be borne out by the changes that occur in the amplitudes at the different frequencies when the voltage is turned off. Such data were not taken by Wettling and Bruun, but were taken by Zucker and Zemon[48] on a similar CdS sample and by Spears[45] and Palik and Bray[50] on GaAs samples. In all three of these references there are data on the changes occurring when the voltage was turned off after $f_{mi}$ had been downshifted by about a factor of 5 from an initial value of about 3 GHz. For 0.6 GHz all three find

that, after a very small fraction of a microsecond in which its amplitude remains more or less constant or continues to grow slowly,[51] there is a region of steep decay. The decay rate is much steeper than that due to lattice attenuation at this frequency. The steep decay persists for about 0.5 $\mu$sec, after which there is a transition to the slower rate expected for lattice attenuation. A similar decay pattern is reported by Spears[45] and Palik and Bray[50] for frequencies in the neighborhood of 1 GHz. For 3 GHz, on the other hand, it is found[48,50] that attenuation does start at once upon turnoff, but that for a period of about 1 $\mu$sec the rate is smaller than that expected for lattice attenuation at this frequency. After this period the expected lattice attenuation appears. Zucker and Zemon[48] find for their sample that the slower initial rate is common to all frequencies above about 1.5 or 2 GHz. The periods of anomalously rapid decay in the 0.6–1-GHz range more or less coincide with those of the anomalously slow decay at the higher frequencies. As pointed out and partially explained by Bray[47] and by Palik and Bray,[50] during these anomalous periods there must be a net conversion of flux from low to high frequencies. We can suggest a more detailed explanation in terms of the picture of the mixing in the domain at this state that was presented earlier. When the voltage is shut off the linear gain ceases. This affects the high frequencies most strongly, because they have appreciable linear gains and lattice attenuation rates. The amplitudes of the coherent waves at the high frequencies begin to drop off at once. Since the downconversion depends exponentially on these amplitudes, the rate of generation of lower frequencies begins to drop off even more rapidly. The rate at which the lower frequencies, such as 0.6 GHz, lose energy by upconversion is less affected, however, since it depends on $|\hat{S}_\omega|^2$ for SecHG or linearly on $|\hat{S}_\omega|$ for upconversion by mixing with another frequency. Thus the balance between downconversion and upconversion is upset and, plausibly, the low frequencies convert energy to the higher frequencies during the anomalous period.

Palik and Bray[50] give evidence that upconversion through interaction with higher frequencies is more important than SecHG. Specifically, they find that the time at which the fast decay at 0.6 GHz makes a transition to the normal lattice decay seems to be more dependent on the presence of some critical level of flux at the higher frequencies than upon its own intensity level. The fact that upconversion through interaction of 0.6 GHz with higher frequencies is a more important process than SecHG at 0.6 GHz is not difficult to understand. For generation of a sum frequency $\omega+\omega'$ we may write a relation similar to (5.6) for generation of $2\omega$, with the quantity

$$G(\omega,\omega')\equiv|\mathcal{A}|k_{\omega+\omega'}/[(\alpha_{\omega+\omega'}-\alpha_{\omega'}-\alpha_\omega)^2+(\Delta k)^2]^{1/2}$$

playing a role analogous to that of $G(2\omega)$. If $\omega$ is taken to be 0.6 GHz and $\omega'$ a frequency in the range 0.6 GHz $\leq\omega'\leq$ 3 GHz, $G(\omega,\omega')$ will by our calculations be greater than $G(2\omega)$ by a factor of about 2 to 5. This advantage in generating $\omega+\omega'$ over generating $2\omega$ will be largely offset or even overcome, by the fact that $|\hat{S}_\omega(0)\hat{S}_{\omega'}(0)|<|\hat{S}_\omega(0)|^2$ since the intensity is a maximum around 0.6 GHz. Even allowing for the fact that $\Delta k$ is likely to be smaller in the high-flux domain, we expect that the probabilities of generating $\omega+\omega'$ and $2\omega$ will be, at best, about equal. It must be remembered, however, that there are very many possibilities for $\omega'$. With this as a weighting factor, it is to be expected that, at 0.6 GHz, more energy will be lost in generation of sum frequencies than in SecHG.

## IV. SUMMARY

For downconversion under constant pump strain the signal and idler amplitudes vary exponentially with $x$, the argument of the exponential including terms involving the pump strain and the difference of the linear gains or losses of signal and idler. In the non-phase-matched case the argument also includes $\Delta k$, while in the phase-matched case it includes angular factors. If the pump is undergoing linear gain or loss at a rate $\alpha_3$ the strain that appears in the exponential is smaller or larger, respectively, than the local pump strain by an amount depending on $\alpha_3$ and $x$. In the absence of trapping, signal gain, except for very small pump intensities or very high pump frequencies, peaks at the subharmonic. Maximum gain at the subharmonic occurs for a pump frequency a little greater than $f_{mg}$. The gain is found to have a local minimum for the dc field at which $v_d=v_s$. For low frequencies $[(\omega/\omega_D)^2\ll\gamma^2]$ this minimum may be quite deep, although narrow. In the presence of trapping the minimum is shifted to $v_d>v_s$. Corresponding to this, the total (linear plus parametric) gain rate for low frequencies shows a deep local minimum for $v_d=v_s$ with no trapping, for $v_d>v_s$ with trapping. Usually, although not always, the gain values are smaller when trapping is included, all other parameters being held the same. For shear waves in the basal plane of CdS phase-matched gain is very strongly favored over collinear at strains of $2\times10^{-5}$ and below. The advantage of phase matching is generally much less at strains greater than $6\times10^{-5}$, how much less depending somewhat on the value of $v_d/v_s$. This is particularly true at high frequencies, where the mismatch in wave vectors depends strongly on $v_d/v_s$.

In upconversion, whether collinear or not, the amplitude of the sum frequency $f_3$ generated from $f_1+f_2$ is not exponential in the strains at $f_1$ and $f_2$

but rather proportional to their product. It also includes a group of exponential factors involving $\alpha_1$, $\alpha_2$, $\alpha_3$, and $\Delta k$ which at small $x$ gives oscillations, but at large enough $x$ becomes essentially either $e^{-\alpha_3 x}$ or $e^{-(\alpha_1+\alpha_2)x}$. The remaining factor, for the case of secHG, peaks for a fundamental frequency equal to $f_{mg}$ and falls off much less rapidly with decreasing frequency than the gain rate for downconversion.

Comparison of the second-order theory derived in this paper with experiments of Zemon and Zucker in which a 1-GHz pump generated subharmonics and second harmonics in CdS indicates that theory can explain the amount of gain observed provided strains are somewhat larger than were estimated. The theory can also account for the variation of pump intensity with distance.

Another conclusion that can be drawn from these experiments and comparison with theory is that large bunching effects predicted by many authors will be much diminished, practically, because of the energy losses that occur in mixing with other frequencies. This appears to apply also to moving domains, where second-order theory can account qualitatively for the downshifting of the frequency of maximum intensity and for the upconversion observed, particularly after removal of the dc field.

## ACKNOWLEDGMENTS

We are grateful to S. Zemon and J. Zucker for valuable discussions of their experimental data and critical readings of the manuscript, and to R. Bray for preprints of his work.

---

[1]D. L. White, J. Appl. Phys. 33, 2547 (1962); A. R. Hutson and D. L. White, *ibid.* 33, 40 (1962).

[2]A theory of parametric amplification for arbitrary strain amplitudes has been presented by Yu. V. Gulayev and P. E. Zilberman, Phys. Letters 30A, 378 (1969).

[3]This relation was derived previously by E. A. Zabolotskaya, S. I. Soluyan, and R. V. Khokhlov, Sov. Phys. Acoust. 12, 380 (1967).

[4]A. K. Ganguly and E. M. Conwell, Phys. Letters 29A, 221 (1969).

[5]C. A. A. J. Greebe, Phys. Letters 4, 45 (1963).

[6]I. Uchida, T. Ishiguro, Y. Sasaki, and T. Suzuki, J. Phys. Soc. Japan 19, 674 (1964).

[7]A. R. Moore and R. W. Smith, Phys. Rev. 138, A1250 (1965).

[8]C. Krischer and U. Ingard, Phys. Letters 32A, 41 (1970), who derived a relation similar to (3.3), have shown that for $\vec{v}_d$ opposite to the wave propagation direction $v_s$ can exceed the stiffened velocity when trapping is present.

[9]This equation, for $\theta_m = 0$, was given by P. D. Southgate and H. N. Spector, J. Appl. Phys. 36, 3728 (1965).

[10]J. A. Armstrong, N. Bloembergen, J. Ducuing, and P. S. Pershan, Phys. Rev. 127, 1918 (1962).

[11]See, for example, R. W. Terhune and P. D. Maker, *Nonliner Optics*, in Vol. 2 of *Lasers*, edited by A. K. Levine (Dekker, New York, 1968), p. 324.

[12]N. Bloembergen, *Nonlinear Optics* (Benjamin, New York, 1965).

[13]Yu. V. Gulyaev and P. E. Zil'berman, Zh. Eksperim. i Teor. Fiz. Pis'ma v Redaktsiya 11, 421 (1970) [Sov. Phys. JETP Letters 11, 286 (1970)].

[14]V. K. Komar and B. L. Timan, Fiz. Tverd. Tela 12, 304 (1970) [Sov. Phys. Solid State 12, 248 (1970)].

[15]N. Bloembergen, Ref. 11, p. 99.

[16]This type of solution was obtained earlier for the case of a longitudinal pump and transverse, degenerate signal, and idler by Zabolotskaya *et al.*, Ref. 3.

[17]J. M. Manley and H. E. Row, Proc. IRE 47, 2115 (1959).

[18]S. Zemon, Phys. Letters 13A, 57 (1970).

[19]S. Zemon (private communication).

[20]A. K. Ganguly, Solid State Commun. 8, 783 (1970).

[21]S. Zemon, J. Zucker, J. H. Wasko, E. M. Conwell, and A. K. Ganguly, Appl. Phys. Letters 12, 378 (1968).

[22]R. Mauro and W. C. Wang, Phys. Rev. B 1, 683 (1970).

[23]SecHG has been treated earlier in similar fashion by H. Kroger, Appl. Phys. Letters 4, 190 (1964); and B. Tell, Phys. Rev. 136, A772 (1964). Note that their solution and ours assumes a boundary condition $\hat{u}_{2\omega}(0) = 0$. If instead we had chosen the boundary condition $u_{2\omega}(0) = \mathcal{C}[\hat{S}_\omega(0)]^2/2(\alpha_{2\omega} - 2\alpha_\omega - i\Delta k)$, we would have obtained what P. N. Butcher [J. Phys. C 4, 36 (1971)] calls a "natural solution," i.e., one without a free second harmonic. In that case our remarks about interference between free and forced waves would, of course, not be applicable.

[24]See, for example, V. L. Gurevich and B. D. Laikhtman, Zh. Eksperim. i Teor. Fiz. 46, 598 (1963) [Sov. Phys. JETP 19, 407 (1964)].

[25]See Yu. V. Gulyaev, Fiz. Tekh. Poluprov. 2, 628 (1968) [Sov. Phys. Semicond. 2, 525 (1968)]; and R. Katilyus, Fiz. Tverd. Tela 10, 458 (1968) [Sov. Phys. Solid State 10, 359 (1968)].

[26]The method of solution and the resulting solutions are similar to those for the corresponding optical case. See N. Bloembergen, Ref. 12, p. 88.

[27]J. Zucker, S. Zemon, E. M. Conwell, and A. K. Ganguly, in *Proceedings of the International Conference on Light Scattering Spectra of Solids*, 1968, edited by G. B. Wright (Springer-Verlag, New York, 1969), p. 615.

[28]S. Zemon and J. Zucker, IBM J. Res. Develop. 13, 494 (1969).

[29]For further discussion see Ref. 28.

[30]L. L. Hope, Phys. Rev. 166, 883 (1968).

[31]R. W. Dixon, J. Appl. Phys. 38, 5149 (1967).

[32]W. T. Maloney and H. R. Carleton, IEEE Trans. Sonics Ultrasonics SU-14, 135 (1967).

[33]V. L. Gurevich, Sov. Phys. Semicond. 2, 1299 (1969). This gives references to earlier work.

[34]P. K. Tien, Phys. Rev. 171, 970 (1968).

[35]P. N. Butcher and N. R. Ogg, J. Phys. C 3, 706 (1970). This gives reference to earlier work.

[36]Yu. V. Gulayev, IEEE Trans. Sonics Ultrasonics SU-17, 111 (1970).

[37]B. K. Ridley, J. Phys. C 3, 935 (1970).

[38]An exception to this is the case of acoustic surface waves on CdS where, as disucssed earlier, for reasons

not yet entirely understood, downconversion effects are weak. See Ref. 18.

[39]E. P. Garshka, V. I. Samulionis, B.-P. P. Ketis, and A. S. Zhyulpa, Fiz. Tverd. Tela 10, 611 (1968) [Sov. Phys. Solid State 10, 480 (1968)]. This includes references to earlier work.

[40]M. Schulz and B. K. Ridley, Phys. Letters 29A, 17 (1969).

[41]J. Zucker and S. Zemon, Appl. Phys. Letters 9, 398 (1966).

[42]For an over-all description and extensive references see N. I. Meyer and M. H. Jorgensen, in *Festkörper Probleme X*, edited by O. Madelung (Vieweg, Braunschweig, Germany, 1970), p. 21.

[43]A. R. Hutson, Phys. Rev. Letters 9, 926 (1962).

[44]W. Wettling and M. Bruun, Phys. Status Solidi 34, 221 (1969).

[45]D. L. Spears, Phys. Rev. B 2, 1931 (1970).

[46]M. Bruun, W. Wettling, and N. I. Meyer, Phys. Letters 31A, 31 (1970).

[47]R. Bray, in *Proceedings of the Tenth International Conference on the Physics of Semiconductors*, edited by S. P. Keller, J. C. Hensel, and F. Stern (Atomic Energy Commission, Oak Ridge, Tenn., 1970), p. 705.

[48]J. Zucker and S. Zemon, J. Phys. Chem. Solids 31, 1673 (1970).

[49]D. S. Zoroglu and I-C. Chang, J. Appl. Phys. 41, 2294 (1970).

[50]E. D. Palik and R. Bray, Phys. Rev. (to be published).

[51]The latter effect, indicating continued downconversion, was reported also by G. I. Robertson and M. B. N. Butler, Electronics Letters 5, 529 (1969).

PHYSICAL REVIEW B VOLUME 4, NUMBER 8 15 OCTOBER 1971

# Neutron Scattering Investigation of Impurity Phonon Modes in Ge(9.2% Si)†

N. Wakabayashi, R. M. Nicklow, and H. G. Smith
*Solid State Division, Oak Ridge National Laboratory Oak Ridge, Tennessee* 37830
(Received 1 March 1971)

The frequencies of the local modes in a Ge single crystal containing 9.2 at.% Si have been measured. A $\vec{Q}$ dependence of the local-mode frequencies has been observed, contrary to the prediction of the isolated mass-defect theory. The theory of Elliott and Taylor gives values for the local-mode frequencies that are in good agreement with the present results. The changes of the in-band mode frequencies of the longitudinal branch along the [001] direction were also measured and the results were in reasonable agreement with the theory.

The frequencies of the local modes and of some in-band modes in a Ge single crystal containing 9.2 at.% Si have been measured by coherent inelastic neutron scattering. The experiments were performed using a triple-axis spectrometer at the HFIR. The sample crystal[1] is a 25-mm-long cylinder having a loaf-shape cross section with maximum and minimum diameters of 15 and 10 mm, respectively. The lattice constant determined from the neutron Bragg reflections is 5.630 Å, which is in good agreement with the result of Dismukes *et al.*[2] Constant-$\vec{Q}$ measurements were made with the scattered neutron energy $E'$ fixed usually at a value corresponding to a frequency of 6.0 THz, although in order to check certain results some measurements were carried out with an $E'$ of 7.0 THz. All of the measurements described here were obtained with the neutron momentum transfer $\hbar\vec{Q}$ along the [001] direction. The scattered neutron groups that were obtained in measurements of the local-mode frequency for two different points in the reciprocal space are shown in Fig. 1.

The similarity of the phonon dispersion curves for Ge[3] and Si[4] suggests that a theory of the lattice dynamics of this alloy which includes only the mass change might be a good approximation. The theory for an isolated mass defect[5] gives a unique value of 11.25 THz for the local-mode frequency $\nu_l$, which is independent of $\vec{Q}$. However, Fig. 1 clearly shows a substantial difference in the local-mode peak positions for two different values of $\vec{Q}$, and the frequencies measured are larger than those given by the isolated mass-defect theory.

Several recent theoretical treatments of the mass-defect problem attempt to take into account the effects of a finite impurity concentration.[6-8] In the present paper we shall compare our results with the theory of Elliott and Taylor.[6] Although this theory is considered to be inadequate in many respects,[7,8] the computations required in making a comparison with experiment are more easily carried out and it does provide a surprisingly good description of the present results.

In this theory, the local-mode frequency is determined by the equation

$$\epsilon\nu_l^2\int \frac{g(\nu)}{\nu_l^2-\nu^2}\,d\nu=\left(1-\frac{c\epsilon\nu_l^2}{\nu_l^2-\nu_j^2(\vec{q})}\right)\frac{1}{1-c}\,, \quad (1)$$

where $c$ is the impurity concentration, $\nu_j(\vec{q})$ is the in-band mode frequency of the unperturbed lattice with wave vector $\vec{q}$ and branch index $j$, $g(\nu)$ is the frequency distribution function, and $\epsilon=1-(M_i/M_h)$, where $M_i$ is the impurity mass and $M_h$ is the host mass. Since in the present work the measurements